

Inferring the non-linear dynamics of stochastic inertial systems

David B. Brückner,^{1,*} Pierre Ronceray,^{2,*} and Chase P. Broedersz^{1,†}

¹*Arnold Sommerfeld Center for Theoretical Physics and Center for NanoScience, Department of Physics, Ludwig-Maximilian-University Munich, Theresienstr. 37, D-80333 Munich, Germany*

²*Center for the Physics of Biological Function, Princeton University, Princeton, NJ 08544, USA*

Many complex systems, ranging from migrating cells to interacting swarms, exhibit effective inertial dynamics described by second order stochastic differential equations. Inferring such an equation of motion from experiments can provide profound insight into the physical laws governing the system. Currently, a general method to reliably infer inertial dynamics from realistic experimental trajectories – sampled at discrete times and subject to measurement noise – is lacking. Here, we derive a principled framework to infer the deterministic and stochastic fields from realistic trajectories of inertial systems with multiplicative noise. Our framework yields an operational method, termed Stochastic Inertial Force Inference, which performs well on experimental trajectories of single migrating cells and in complex high-dimensional systems including flocks with Viscek-like alignment interactions.

Across the scientific disciplines, data-driven methods are used to unravel the dynamics of complex stochastic systems. These approaches often take the form of inverse problems, with the aim to derive the underlying governing equation of motion from observed trajectories. This problem is now well understood in overdamped systems which are governed by first-order stochastic differential equations, such as Brownian dynamics [1–6]. Many complex systems however exhibit effective inertial dynamics, and thus require a second-order description. Examples include cell motility [7–13], postural dynamics in animals [14, 15], movement in interacting swarms of fish [16–18], birds [19, 20], and insects [21, 22], as well as dynamics in granular media [23] and plasmas [24]. However, a general method to reliably infer the dynamics of stochastic inertial systems has remained elusive.

Inference from inertial trajectories suffers from a major challenge that does not exist in overdamped systems. In any realistic application, the accelerations of the degrees of freedom must be obtained as discrete second derivatives from the observed position trajectories, which are sampled at a finite time interval Δt . Consequently, a straightforward generalisation of the estimators for the deterministic and stochastic contributions to the dynamics commonly used in first-order systems fails: these estimators do not converge to the correct values, even in the limit $\Delta t \rightarrow 0$, a key issue that was recently observed in linear inertial systems [25, 26]. To make matters worse, real data is always subject to measurement noise, leading to divergent terms in the discrete estimators, implying that even very small amplitude noise can make accurate inference impossible [27]. These problems have so far precluded reliable inference in inertial systems.

Here, we introduce a general framework, Stochastic Inertial Force Inference (SIFI), that conceptually explains the origin of these divergent biases, and provides an operational scheme to reliably infer inertial dynamics in non-linear systems with multiplicative noise. To provide a method that can be robustly applied to realistic ex-

perimental data sets, consisting of discrete trajectories subject to measurement noise, we rigorously derive estimators which converge to the correct values for such data. Furthermore, we provide a practical tool to perform model selection that reveals the dominant components of the inferred dynamics, based on how much information about the force field these components capture. We demonstrate the power of our method by applying it to short experimental trajectories of single migrating cells on confining micropatterns, as well as simulated complex high-dimensional data sets, including flocks of active particles with Viscek-style alignment interactions.

We consider a general d -dimensional stationary inertial process $x_\mu(t)$ governed by equations of the general form

$$\begin{aligned}\dot{x}_\mu &= v_\mu \\ \dot{v}_\mu &= F_\mu(\mathbf{x}, \mathbf{v}) + \sigma_{\mu\nu}(\mathbf{x}, \mathbf{v})\xi_\nu(t)\end{aligned}\quad (1)$$

where $\xi_\mu(t)$ represents a Gaussian white noise with the properties $\langle \xi_\mu(t)\xi_\nu(t') \rangle = \delta_{\mu\nu}\delta(t-t')$ and $\langle \xi_\mu(t) \rangle = 0$. We interpret Eq. (1) in the Itô-sense throughout, and thus infer the force field $F(\mathbf{x}, \mathbf{v})$ corresponding to this convention. Our aim is to infer the dynamical terms $F_\mu(\mathbf{x}, \mathbf{v})$ and $\sigma_{\mu\nu}(\mathbf{x}, \mathbf{v})$ from an observed trajectory of the process.

We start by approximating the force field as a linear combination of n_b basis functions $b = \{b_\alpha(\mathbf{x}, \mathbf{v})\}_{\alpha=1\dots n_b}$, such as polynomials, Fourier modes, wavelet functions, or Gaussian kernels [14]. From these basis functions, we construct an empirical orthonormal basis $\hat{c}_\alpha(\mathbf{x}, \mathbf{v}) = \hat{B}_{\alpha\beta}^{-1/2}b_\beta(\mathbf{x}, \mathbf{v})$ such that $\langle \hat{c}_\alpha\hat{c}_\beta \rangle = \delta_{\alpha\beta}$, an approach that was recently proposed for overdamped systems [6]. Here and throughout, averages correspond to time-averages along the trajectory. We can then approximate the force field as $F_\mu(\mathbf{x}, \mathbf{v}) \approx F_{\mu\alpha}\hat{c}_\alpha(\mathbf{x}, \mathbf{v})$. Similarly, we perform a basis expansion of the stochastic term $\sigma_{\mu\nu}^2(\mathbf{x}, \mathbf{v})$. Thus, the inference problem reduces to estimating the projection coefficients $F_{\mu\alpha}$ and $\sigma_{\mu\nu\alpha}^2$.

We first focus on the case without measurement noise. Here, the challenge is to deal with the discreteness of the observed data: in experiments, only the configurational

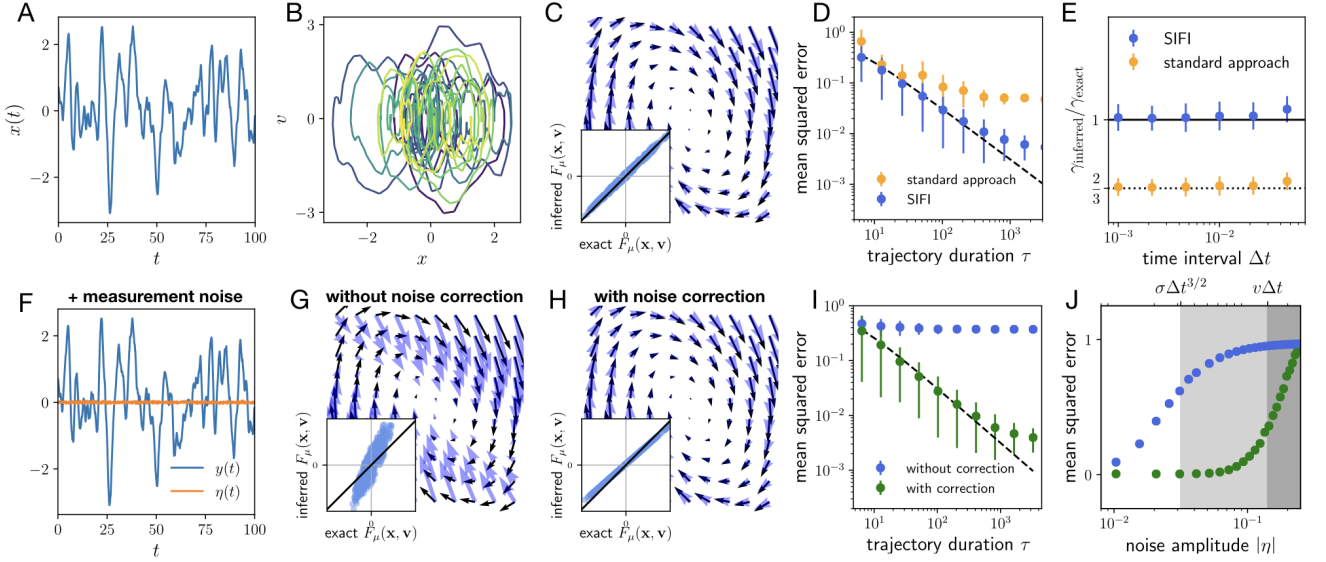


FIG. 1. **Damped harmonic oscillator.** **A.** Trajectory $x(t)$ of a stochastic damped harmonic oscillator, $F(x, v) = -\gamma v - kx$. **B.** The same trajectory represented in xv -phase space. Color coding indicates time. **C.** Force field in xv -space inferred from the trajectory in A using SIFI with basis functions $b = \{1, x, v\}$ (blue arrows), compared to the exact force field (black arrows). *Inset:* inferred components of the force along the trajectory *versus* the exact values. **D.** Convergence of the mean squared error of the inferred force field, obtained using SIFI (blue) *versus* with the previous standard approach [11, 14, 25, 27] (orange). Dashed lines indicate the theoretical predictions of the errors. **E.** Inferred divided by exact friction coefficient γ as a function of the sampling time interval Δt , comparing the previous standard approach to SIFI. **F.** Noisy trajectory $y(t) = x(t) + \eta(t)$ (blue) corresponding to the same realization $x(t)$ as in panel A, with additional time-uncorrelated measurement noise $\eta(t)$ (orange) with a small amplitude $|\eta| = 0.02$. **G, H.** Force field inferred from the noisy trajectory in F using estimators without and with measurement noise corrections, respectively. **I.** Convergence curves for inference from data subject to measurement noise using estimators without (blue) and with (green) measurement noise corrections. **J.** Dependence of the mean squared error on the noise amplitude $|\eta|$, with the same symbols as in I.

coordinate $\mathbf{x}(t)$ is observed, and is sampled at a discrete time-interval Δt . We therefore only have access to the discrete estimators of the velocity $\hat{\mathbf{v}}(t) = [\mathbf{x}(t) - \mathbf{x}(t - \Delta t)]/\Delta t$ and acceleration $\hat{\mathbf{a}}(t) = [\mathbf{x}(t + \Delta t) - 2\mathbf{x}(t) + \mathbf{x}(t - \Delta t)]/\Delta t^2$. Thus, we need to derive an estimator $\hat{F}_{\mu\alpha}$, constructed from the discrete velocities and accelerations, which converges to the exact projections $F_{\mu\alpha}$ in the limit $\Delta t \rightarrow 0$.

An intuitive estimator for the force projections $\hat{F}_{\mu\alpha}$ would be to simply generalize the approach to overdamped systems [6] and calculate the projections of the accelerations $\langle \hat{a}_\mu \hat{c}_\alpha(\mathbf{x}, \hat{\mathbf{v}}) \rangle$. This expression has indeed previously been used for inertial systems [11, 14, 25, 27]. Our projection-based formalism allows us to derive the correction term to this estimator for a general process of the form in Eq. (1), by expanding the basis functions: $c_\alpha(\mathbf{x}, \hat{\mathbf{v}}) = c_\alpha(\mathbf{x}, \mathbf{v}) + (\partial_{v_\mu} c_\alpha)(\hat{v}_\mu - v_\mu) + \dots$. Here, the leading order contribution to the second term is a fluctuating (zero average) term of order $\Delta t^{1/2}$. Similarly, we perform a stochastic Itô-Taylor expansion of the discrete acceleration $\hat{\mathbf{a}}(t)$, which has a leading order fluctuating term of order $\Delta t^{-1/2}$. Thus, while each of these terms individually averages to zero, their product results in a non-zero average contribution of order Δt^0 : $\langle \hat{a}_\mu \hat{c}_\alpha(\mathbf{x}, \hat{\mathbf{v}}) \rangle =$

$F_{\mu\alpha} + \frac{1}{6} \langle \sigma_{\mu\nu}^2 \partial_{v_\nu} c_\alpha(\mathbf{x}, \mathbf{v}) \rangle + \mathcal{O}(\Delta t)$ [28]. This is the general expression for the $\mathcal{O}(\Delta t^0)$ bias recently observed in the specific case of linear systems [25, 26]. Specifically, for a linear viscous damping force $F(v) = -\gamma v$, it was found that $\langle \hat{a}c(\hat{v}) \rangle = -\frac{2}{3}\gamma + \mathcal{O}(\Delta t)$, which is recovered by our general expression for the $\mathcal{O}(\Delta t^0)$ bias [28]. Our derivation thus shows that this systematic bias poses a problem more generally wherever a second derivative of a stochastic signal is averaged conditioned on its first derivative.

Previous approaches to correct for this bias rely on an explicit solution and *a priori* knowledge of the observed stochastic process [25], are limited to linear systems with constant noise [26], or perform an *a posteriori* empirical iterative scheme [11]. In contrast, our formalism yields a general unbiased estimator for the force projections, by simply deducting the bias [28]:

$$\hat{F}_{\mu\alpha} = \langle \hat{a}_\mu \hat{c}_\alpha(\mathbf{x}, \hat{\mathbf{v}}) \rangle - \frac{1}{6} \left\langle \widehat{\sigma}_{\mu\nu}^2(\mathbf{x}, \hat{\mathbf{v}}) \partial_{v_\nu} \hat{c}_\alpha(\mathbf{x}, \hat{\mathbf{v}}) \right\rangle \quad (2)$$

The appearance of the derivative of a basis function in the estimator highlights the importance of projecting the dynamics of second order systems onto a set of *smooth* basis functions, in contrast to the traditional approach of

taking conditional averages in a discrete set of bins [1, 2], which is equivalent to using a basis of non-differentiable top-hat functions.

Importantly, Eq. (2) implies that the stochastic term has to be inferred before the deterministic estimator can be evaluated. Similarly to the force field, we can expand the stochastic term as a sum of basis functions, and derive an unbiased estimator for the projection coefficients [28]

$$\widehat{\sigma^2}_{\mu\nu\alpha} = \frac{3\Delta t}{2} \langle \hat{a}_\mu \hat{a}_\nu \hat{c}_\alpha(\mathbf{x}, \hat{\mathbf{v}}) \rangle \quad (3)$$

We test our method on a simulated trajectory of the stochastic damped harmonic oscillator, $\dot{v} = -\gamma v - kx + \sigma\xi$ (Fig. 1A-D). As expected, the acceleration projections $\langle \hat{a}_\mu \hat{c}_\alpha(\mathbf{x}, \hat{\mathbf{v}}) \rangle$ yield a biased estimator (Fig. 1E). In contrast, SIFI, defined by Eqs. (3) and (2), provides an accurate reconstruction of the force field (Fig. 1C,E) [29]. To test the convergence of these estimators in a quantitative way, we calculate the expected random error due to the finite length τ of the input trajectory, $\delta\hat{F}^2/\hat{F}^2 \sim N_b/2\hat{I}_b$, where we define $\hat{I}_b = \frac{\tau}{2} \hat{\sigma}_{\mu\nu}^{-2} \hat{F}_{\mu\alpha} \hat{F}_{\nu\alpha}$ as the empirical estimate of the information contained in the trajectory, and $N_b = dn_b$ is the number of degrees of freedom in the force field [6]. We confirm that the convergence of our estimators follows this expected trend, in contrast to the biased acceleration projections (Fig. 1D). Therefore, SIFI provides an operational method to accurately infer the dynamical terms of inertial trajectories.

A key challenge in stochastic inference from real data is the unavoidable presence of time-uncorrelated measurement noise $\boldsymbol{\eta}(t)$, which can be non-Gaussian: the observed signal in this case is $\mathbf{y}(t) = \mathbf{x}(t) + \boldsymbol{\eta}(t)$. This problem is particularly dominant in inertial inference, where the signal is differentiated twice, such that even a very small noise amplitude leads to large errors in the inferred force field, prohibiting accurate inference from the data in most cases. In fact, the force estimator (Eq. (2)) includes a divergent bias of order Δt^{-3} , which dominates all other errors for small Δt [28]; this cannot be rectified by simply recording more data.

To overcome this challenge, we derive unbiased estimators which are robust against measurement noise. These estimators are constructed in such a way that the leading-order noise-induced bias terms cancel out. For the force estimator, we find that this is achieved by using the local average position $\bar{\mathbf{x}}(t) = \frac{1}{3}(\mathbf{x}(t - \Delta t) + \mathbf{x}(t) + \mathbf{x}(t + \Delta t))$ and the symmetric velocity $\hat{\mathbf{v}}(t) = [\mathbf{x}(t + \Delta t) - \mathbf{x}(t - \Delta t)]/(2\Delta t)$ in Eq. (2). Note that due to the change of definition of $\hat{\mathbf{v}}$, the prefactor of the correction term in Eq. (2) changes by a factor 3. Similarly, we derive an unbiased estimator for the stochastic term, which is constructed using a linear combination of four-point increments [28].

Remarkably, these modifications to the estimators result in a vastly improved inference performance in the presence of measurement noise (Fig. 1F-J), where the

standard estimators fail dramatically. Specifically, while the bias becomes dominant at a noise magnitude $|\eta| \sim \sigma\Delta t^{3/2}$ in the standard estimators, the bias-corrected estimators fail when the noise magnitude becomes comparable to the displacement in a single time-step, $|\eta| \sim v\Delta t$ (Fig. 1J) [28]. Thus, our method has a significantly larger range of validity up to measurement noise amplitudes as large as the typical displacement in a single time-frame. In situations where $|\eta|$ exceeds this threshold, we propose to simply employ local time-averaging until Δt is large enough and $|\eta|$ is small enough for SIFI to perform well.

In the previous example, we have focused on a simple system with a linear force field. However, in many complex systems the force field is highly non-linear [11, 14]. Since our method does not assume linearity, we can simply expand the projection basis to include higher order polynomials, or other appropriate non-linear basis sets. As a canonical example, we study the stochastic Van der Pol oscillator $\dot{v} = \mu(1 - x^2)v - x + \sigma\xi$. Such non-linear relaxation oscillators appear in a broad range of biological dynamical systems [31]. We simulate a short trajectory of this process, with added artificial measurement noise (Fig. 2A). Indeed, we find that SIFI reliably infers the underlying phase-space flow (Fig. 2B). Importantly, this good performance does not rely on using a polynomial basis to fit polynomial forces: employing a non-adapted basis of Fourier components yields similarly good results [28].

To capture the Van der Pol dynamics, only the three basis functions $\{x, v, x^2v\}$ are required. But can these functions be identified directly from the data without prior knowledge of the underlying model? To address this question, we employ the concept of partial information. We can estimate the information contained in a finite trajectory as $\hat{I}_b(n_b) = \frac{\tau}{2} \hat{\sigma}_{\mu\nu}^{-2} \hat{F}_{\mu\alpha} \hat{F}_{\nu\alpha}$, where $\hat{F}_{\nu\alpha}$ are the projection coefficients onto the basis b with n_b basis functions [6]. Our aim is to maximize the information captured by the force field. Thus, to assess the importance of the n^{th} basis function in the expansion, we calculate the amount of information it adds to the inferred force field:

$$\hat{I}_b^{(\text{partial})}(n) = \hat{I}_b(n) - \hat{I}_b(n-1) \quad (4)$$

which we term the partial information contributed by the basis function b_n . Indeed, if we project the Van der Pol dynamics onto a large number of basis functions, such as a polynomial basis of order 6, the partial information peaks at only 3 out of 28 basis functions, corresponding to $\{x, v, x^2v\}$ (Fig. 2C). Thus, the partial information provides a useful heuristic for detecting the relevant terms of the deterministic dynamics.

To illustrate that SIFI is practical and data-efficient, we apply it to experimental trajectories of cells migrating in a two-state confinement (Fig. 2D). Within their life-time, these cells perform several transitions between the two states, resulting in relatively short trajectories.

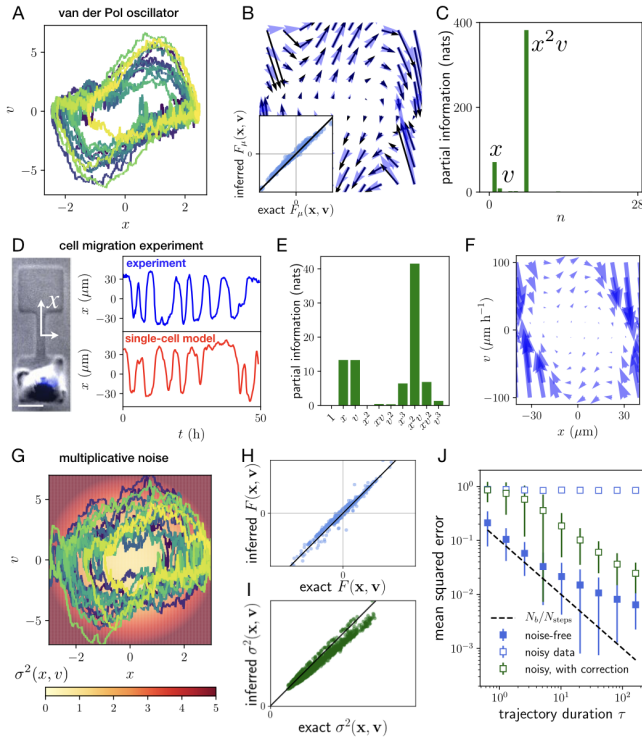


FIG. 2. Inferring non-linear dynamics and multiplicative noise. **A.** xv -trajectory of the stochastic Van der Pol oscillator [30], $F(x, v) = \mu(1 - x^2)v - x$, with measurement noise. **B.** SIFI applied to the trajectory in A allows precise reconstruction of the force field, projected here on a polynomial basis expansion to order 6. **C.** Partial information of the 28 functions in the 6th order polynomial basis in natural information units (1 nat = $1/\log 2$ bits). **D.** Microscopy image of a migrating human breast cancer cell (MDA-MB-231) confined in a two-state micropattern, the nucleus is marked in blue (scale bar: $20\mu\text{m}$). Experimental trajectory of the cell nucleus position, recorded at a time-interval $\Delta t = 10$ h (blue), and trajectory predicted by the model inferred from this trajectory (red). **E.** Partial information for the experimental trajectory in D, projected onto a third-order polynomial basis. **F.** Deterministic flow field inferred from the experimental trajectory in D. **G.** Trajectory of a Van der Pol oscillator with multiplicative noise $\sigma^2(x, v) = \sigma_0 + \sigma_x x^2 + \sigma_v v^2$ (colormap), with measurement noise. **H, I.** Inferred *versus* exact components of the force and diffusion term, respectively, for the trajectory in G. **J.** Inference convergence of the multiplicative term using Eq. (3) without measurement noise (solid squares), with measurement noise (blue open squares), and using the estimator with noise correction (green open squares). The error saturation at large τ is due to the finite time-step. Dashed line: predicted error $\delta\sigma^2/\sigma^2 \sim \sqrt{N_b\Delta t/\tau}$ [6].

Previously, we inferred dynamical properties by averaging over a large ensemble of trajectories [11]. In contrast, with SIFI, we can reliably infer the dynamics from single cell trajectories. We employ the partial information to guide our basis selection: indeed, the partial information recovers the intrinsic symmetry of the system, suggest-

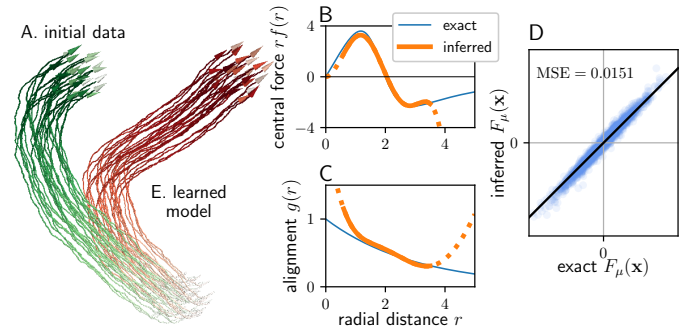


FIG. 3. Interacting flocks. **A.** Trajectory (green) of a group of $N = 27$ Viscek-like particles (Eq. 5) in the flocking regime, with 1000 time points. We perform SIFI on this trajectory using a translation-invariant basis of pair interaction and alignment terms, both fitted with $n = 8$ exponential kernels. **B.** The exact (blue) and inferred (orange) central force $rf(r)$. The exact form is a soft potential with short-range repulsion and long-range attraction, $f(r) = \epsilon_0(1 - (r/r_0)^3)/((r/r_0)^6 + 1)$. The dotted part of the inferred force indicates unreliable extrapolation to distances not sampled by the initial data. **C.** Exact and inferred alignment kernel $g(r)$. The exact form is $g(r) = \epsilon_1 \exp(-r/r_1)$. **D.** Inferred *versus* exact force components along the initial trajectory. **E.** Simulated trajectory (red) employing the inferred force and diffusion fields, with the same initial conditions and total duration as the input data, showing qualitatively similar flocking behavior.

ing a symmetrized third order polynomial expansion is a suitable choice (Fig. 2E). Using this expansion, we infer the deterministic flow field governing the motion, which predicts trajectories very similar to the experimentally observed ones (Fig. 2F). Importantly, the inferred model is self-consistent: re-inferring from short simulated trajectories yields a similar model [28]. Using SIFI, we can thus perform inference on much smaller data sets than previously, and use it for "single-cell profiling", which could provide a useful tool to characterize the intrinsic cell-to-cell variability in the system [13].

To demonstrate the broad applicability of our approach, we evaluate its performance in the presence of multiplicative noise $\sigma_{\mu\nu}(\mathbf{x}, \mathbf{v})$. Indeed, many complex systems exhibit stochastic fluctuations that depend on the state of the system, leading to a multiplicative noise term [11, 14, 32]. SIFI accurately recovers the space- and velocity-dependence of both the deterministic and stochastic term for a system with multiplicative noise, and the estimators converge to the exact values, even in the presence of measurement noise (Fig. 2G-J). To summarize, we have shown that SIFI performs well on short trajectories of non-linear data sets subject to measurement noise, and can accurately infer the spatial structure of multiplicative stochastic terms.

A major challenge in stochastic inference is the treatment of interacting many-body systems. In recent years,

trajectory data on active collective systems, such as bacterial suspensions [33], collective cell migration [34, 35], and swarms of animals [19–22, 36] have become readily available. Previous approaches to such systems frequently focus on the study of correlations [19, 37, 38] or collision statistics [18, 34, 36], but no general method for inferring their underlying dynamics has been proposed. The collective behaviour of these systems, ranging from disordered swarms [22] to ordered flocking [19], is determined by the interplay of active self-propulsion, cohesive and alignment interactions, and noise. Thus, disentangling these contributions could provide key insights into the physical laws governing active collective systems.

We thus consider a simple model for the dynamics of a 3D flock with Viscek-style alignment interactions [39–42], as given by the equation of motion

$$\dot{\mathbf{v}}_i = \mathbf{p}_i + \sum_{j \neq i} [f(r_{ij})\mathbf{r}_{ij} + g(r_{ij})\mathbf{v}_{ij}] + \sigma \boldsymbol{\xi}_i \quad (5)$$

where $\mathbf{r}_{ij} = \mathbf{r}_j - \mathbf{r}_i$, $\mathbf{v}_{ij} = \mathbf{v}_j - \mathbf{v}_i$, and $\mathbf{p}_i = \gamma(v_0^2 - |\mathbf{v}_i|^2)\mathbf{v}_i$ is a self-propulsion force acting along the direction of motion of each particle. Here, f and g denote the strength of the central force and alignment interactions, respectively, as a function of interparticle distance r_{ij} . This model exhibits a diversity of behaviors, including collective flocking (Fig. 3A). Intuitively, one might expect that SIFI should fail dramatically in such a system: in a 3D swarm of N particles, there are $6N$ degrees of freedom, and "curse of dimensionality" arguments might make this problem seem intractable. However, by exploiting symmetries of the system, such as particle exchange symmetry and radial symmetry of the interactions [28], we find that SIFI accurately recovers the r -dependence of the interaction and alignment terms (Fig. 3B-C) and captures the full force field (Fig. 3D). By simulating the dynamics of the inferred model, one obtains new trajectories with high statistical similarity to the original one (Fig. 3E). This example illustrates the potential of SIFI for inferring complex interactions from trajectories of stochastic many-body systems.

In summary, we demonstrate how to reliably infer the deterministic and stochastic components in complex inertial systems. We have shown that the inevitable presence of discreteness and measurement noise result in systematic biases that have so far prohibited accurate inference. To circumvent these problems, we have rigorously derived unbiased estimators, providing an operational framework, Stochastic Inertial Force Inference, to infer stochastic inertial dynamics. Furthermore, we demonstrated how a principled selection of basis functions can yield insights in systems that would otherwise be intractable, such as swarms and flocks of interacting particles. Our method therefore provides a new avenue to analyzing the dynamics of complex high-dimensional systems, such as assemblies of motile cells [34, 35], active swarms [19, 21, 22, 36], as well as non-equilibrium soft

and hard condensed matter systems [23, 24, 31].

We thank Alexandra Fink and Joachim Rädler for generously providing experimental cell trajectories. Funded by the Deutsche Forschungsgemeinschaft (DFG, German Research Foundation) - Project-ID 201269156 - SFB 1032 (Project B12). D.B.B. is supported by a DFG fellowship within the Graduate School of Quantitative Biosciences Munich (QBM) and by the Joachim Herz Stiftung.

* These authors contributed equally.

† c.broedersz@lmu.de

- [1] S. Siegert, R. Friedrich, and J. Peinke, *Phys. Lett. A* **243**, 275 (1998).
- [2] M. Ragwitz and H. Kantz, *Physical Review Letters* **87**, 254501 (2001).
- [3] R. Friedrich, J. Peinke, M. Sahimi, and M. Reza Rahimi Tabar, *Physics Reports* **506**, 87 (2011).
- [4] M. E. Beheiry, M. Dahan, and J. B. Masson, *Nature Methods* **12**, 594 (2015).
- [5] L. Pérez García, J. Donlucas Pérez, G. Volpe, A. V. Arzola, and G. Volpe, *Nature Communications* **9**, 5166 (2018).
- [6] A. Frishman and P. Ronceray, *Phys. Rev. X* (in press), [arXiv:1809.09650](https://arxiv.org/abs/1809.09650) (2020).
- [7] D. Selmececi, S. Mosler, P. H. Hagedorn, N. B. Larsen, and H. Flyvbjerg, *Biophysical Journal* **89**, 912 (2005).
- [8] H. Takagi, M. J. Sato, T. Yanagida, and M. Ueda, *PLoS ONE* **3**, e2648 (2008).
- [9] H. U. Bödeker, C. Beta, T. D. Frank, and E. Bodenschatz, *EPL (Europhysics Letters)* **90**, 28005 (2010).
- [10] L. Li, E. C. Cox, and H. Flyvbjerg, *Physical Biology* **8**, 046006 (2011).
- [11] D. B. Brückner, A. Fink, C. Schreiber, P. J. F. Röttgermann, J. O. Rädler, and C. P. Broedersz, *Nature Physics* **15**, 595 (2019).
- [12] A. Fink, D. B. Brückner, C. Schreiber, P. J. Röttgermann, C. P. Broedersz, and J. O. Rädler, *Biophysical Journal* **118**, 552 (2020).
- [13] D. B. Brückner, A. Fink, J. O. Rädler, and C. P. Broedersz, *J. R. Soc. Interface* **17**, 20190689 (2020).
- [14] G. J. Stephens, B. Johnson-Kerner, W. Bialek, and W. S. Ryu, *PLoS Comput Biol* **4**, e1000028 (2008).
- [15] G. J. Stephens, M. Bueno, D. Mesquita, W. S. Ryu, and W. Bialek, *Proc. Natl. Acad. Sci. USA* **108**, 7286 (2011).
- [16] J. Gautrais, C. Jost, M. Soria, A. Campo, S. Motsch, R. Fournier, S. Blanco, and G. Theraulaz, *Journal of Mathematical Biology* **58**, 429 (2009).
- [17] J. Gautrais, F. Ginelli, R. Fournier, S. Blanco, M. Soria, H. Chaté, and G. Theraulaz, *PLoS Computational Biology* **8** (2012), [10.1371/journal.pcbi.1002678](https://doi.org/10.1371/journal.pcbi.1002678).
- [18] Y. Katz, K. Tunström, C. C. Ioannou, C. Huepe, and I. D. Couzin, *Proceedings of the National Academy of Sciences of the United States of America* **108**, 18720 (2011).
- [19] A. Cavagna, A. Cimarelli, I. Giardina, G. Parisi, R. Santagati, F. Stefanini, and M. Viale, *Proceedings of the National Academy of Sciences* **107**, 11865 (2010).
- [20] A. Attanasi, A. Cavagna, L. Del Castello, I. Giardina,

- T. S. Grigera, A. Jelic, S. Melillo, L. Parisi, O. Pohl, E. Shen, and M. Viale, *Nature Physics* **10**, 691 (2014).
- [21] J. Buhl, D. J. T. Sumpter, I. D. Couzin, J. J. Hale, E. Despland, E. R. Miller, and S. J. Simpson, *Science* **312**, 1402 (2006).
- [22] A. Attanasi, A. Cavagna, L. Del Castello, I. Giardina, S. Melillo, L. Parisi, O. Pohl, B. Rossaro, E. Shen, E. Silvestri, and M. Viale, *PLoS Computational Biology* **10**, e1003697 (2014).
- [23] M. Baldovin, A. Puglisi, and A. Vulpiani, *PLoS ONE* **14**, 1 (2019).
- [24] G. Gogia and J. C. Burton, *Physical Review Letters* **119**, 1 (2017).
- [25] J. N. Pedersen, L. Li, C. Grdinaru, R. H. Austin, E. C. Cox, and H. Flyvbjerg, *Physical Review E* **94**, 062401 (2016).
- [26] F. Ferretti, V. Chardès, T. Mora, A. M. Walczak, and I. Giardina, *arXiv:1912.10491* (2019).
- [27] B. Lehle and J. Peinke, *Physical Review E - Statistical, Nonlinear, and Soft Matter Physics* **91**, 1 (2015).
- [28] See Supplemental Material at [URL will be inserted by publisher] for detailed derivations of the correction terms and estimators.
- [29] A readily usable Python package to perform Stochastic Inertial Force Inference is available at <https://github.com/ronceray/StochasticInertialForceInference>.
- [30] B. van der Pol, *Philos. Mag.* **2**, 978 (1926).
- [31] K. Kruse and F. Jülicher, *Current Opinion in Cell Biology* **17**, 20 (2005).
- [32] R. Friedrich, J. Peinke, and C. Renner, *Physical Review Letters* **84**, 5224 (2000).
- [33] D. T. Chen, A. W. Lau, L. A. Hough, M. F. Islam, M. Goulian, T. C. Lubensky, and A. G. Yodh, *Physical Review Letters* **99**, 148302 (2007).
- [34] J. D'alessandro, A. P. Solon, Y. Hayakawa, C. Anjard, F. Detcheverry, J. P. Rieu, and C. Rivière, *Nature Physics* **13**, 999 (2017).
- [35] A. Palamidessi, C. Malinverno, E. Frittoli, S. Corallino, E. Barbieri, S. Sigismund, G. V. Beznoussenko, E. Martini, M. Garre, I. Ferrara, C. Tripodo, F. Ascione, E. A. Cavalcanti-Adam, Q. Li, P. P. Di Fiore, D. Parazzoli, F. Giavazzi, R. Cerbino, and G. Scita, *Nature Materials* **18**, 1252 (2019).
- [36] R. Lukeman, Y. X. Li, and L. Edelstein-Keshet, *Proceedings of the National Academy of Sciences of the United States of America* **107**, 12576 (2010).
- [37] A. Cavagna, I. Giardina, and T. S. Grigera, *Physics Reports* **728**, 1 (2017).
- [38] W. Bialek, A. Cavagna, I. Giardina, T. Mora, E. Silvestri, M. Viale, and A. M. Walczak, *Proceedings of the National Academy of Sciences* **109**, 4786 (2012).
- [39] Tamas Vicsek, A. Czirok, E. Ben-Jacob, I. Cohen, and O. Shochet, *Phys. Rev. Lett.* **74** (1995).
- [40] G. Grégoire, H. Chaté, and Y. Tu, *Physica D: Nonlinear Phenomena* **181**, 157 (2003).
- [41] H. Chaté, F. Ginelli, G. Grégoire, F. Peruani, and F. Raynaud, *European Physical Journal B* **64**, 451 (2008).
- [42] A. Cavagna, L. Del Castello, I. Giardina, T. Grigera, A. Jelic, S. Melillo, T. Mora, L. Parisi, E. Silvestri, M. Viale, and A. M. Walczak, *Journal of Statistical Physics* **158**, 601 (2014).

Supplementary Material:

Inferring the non-linear dynamics of stochastic inertial systems

David B. Brückner*, Pierre Ronceray* and Chase P. Broedersz

This Supplemental Material contains a detailed definition of the projection formalism we employ in SIFI (section 1), derivations of the unbiased estimators for the deterministic and stochastic terms for discrete data (section 2) and for discrete data with measurement noise (section 3), further details on the inference from experimental single cell trajectories (section 4) and detailed information on the models and parameters used for the simulation results shown in Figs. 1-3 in the main text (section 5).

Contents

1	Definition of the projection formalism	1
2	Derivation of the discrete estimators	2
2.1	Itô integrals	3
2.2	Deterministic term	3
2.3	Stochastic term	5
2.4	Comparison to the exact formula for a linear damping force	6
3	Derivation of estimators in the presence measurement noise	6
3.1	Deterministic term	7
3.2	Stochastic term	8
3.3	Scaling of the inference error with the measurement noise amplitude	13
4	Inference from experimental single cell trajectories	14
4.1	Information content of experimental single cell trajectories	14
4.2	Self-consistency test of the single-cell inference	14
5	Model details and simulation parameters for numerical results	17
5.1	Damped harmonic oscillator (Fig. 1)	17
5.2	Van der Pol oscillator (Fig. 2)	18
5.3	Interacting flocks (Fig. 3)	18

1 Definition of the projection formalism

In SIFI, we approximate the deterministic term as a linear combination of basis functions $b = \{b_\alpha(\mathbf{x}, \mathbf{v})\}$. To extract the coefficients of this functional expansion, we can project the deterministic dynamics onto the space spanned by $b_\alpha(\mathbf{x}, \mathbf{v})$ using the steady-state probability distribution $P(\mathbf{x}, \mathbf{v})$ as a measure [1]. To do so, we define orthonormalized projectors $c_\alpha(\mathbf{x}, \mathbf{v}) = B_{\alpha\beta}^{-1/2} b_\beta(\mathbf{x}, \mathbf{v})$, such that

$$\langle c_\alpha c_\beta \rangle = \int c_\alpha(\mathbf{x}, \mathbf{v}) c_\beta(\mathbf{x}, \mathbf{v}) P(\mathbf{x}, \mathbf{v}) d\mathbf{x} d\mathbf{v} = \delta_{\alpha\beta} \quad (\text{S1})$$

We then approximate the deterministic term as a linear combination of these basis functions

$$F_\mu(\mathbf{x}, \mathbf{v}) \approx F_{\mu\alpha} c_\alpha(\mathbf{x}, \mathbf{v}) \quad (\text{S2})$$

Note that if we use a complete set of basis functions, this becomes an exact equality. The projection coefficients $F_{\mu\alpha}$ are given by

$$F_{\mu\alpha} = \int F_\mu(\mathbf{x}, \mathbf{v}) c_\alpha(\mathbf{x}, \mathbf{v}) P(\mathbf{x}, \mathbf{v}) d\mathbf{x} d\mathbf{v} \quad (\text{S3})$$

Similarly, we expand the stochastic term

$$\sigma_{\mu\nu}^2(\mathbf{x}, \mathbf{v}) \approx \sigma_{\mu\nu\alpha}^2 c_\alpha(\mathbf{x}, \mathbf{v}) \quad (\text{S4})$$

with the projection coefficients

$$\sigma_{\mu\nu\alpha}^2 = \int \sigma_{\mu\nu}^2(\mathbf{x}, \mathbf{v}) c_\alpha(\mathbf{x}, \mathbf{v}) P(\mathbf{x}, \mathbf{v}) d\mathbf{x} d\mathbf{v} \quad (\text{S5})$$

Note that we expand σ^2 rather than σ because we can only derive estimators for σ^2 ; since the noise averages to zero, we must take squares of the increments to extract the magnitude of the fluctuations.

In practice, we aim to infer the deterministic and stochastic terms of the dynamics of a system from a single trajectory of finite length τ , sampled at a time interval Δt . Thus, the exact probability distribution $P(\mathbf{x}, \mathbf{v})$ is unknown, and we cannot enforce the condition Eq. (S1) exactly. Thus, we define *empirical* orthonormalized projectors

$$\hat{c}_\alpha(\mathbf{x}, \mathbf{v}) = \hat{B}_{\alpha\beta}^{-1/2} b_\beta(\mathbf{x}, \mathbf{v}) \quad (\text{S6})$$

where

$$\hat{B}_{\alpha\beta} = \frac{\Delta t}{\tau} \sum_t b_\alpha(\mathbf{x}(t), \mathbf{v}(t)) b_\beta(\mathbf{x}(t), \mathbf{v}(t)), \quad (\text{S7})$$

such that $\langle \hat{c}_\alpha \hat{c}_\beta \rangle = \delta_{\alpha\beta}$ where $\langle \dots \rangle$ refers to a time-average along the observed trajectory.

Our aim in performing inference is to find the terms $F_\mu(\mathbf{x}, \mathbf{v})$ and $\sigma_{\mu\nu}^2(\mathbf{x}, \mathbf{v})$. Thus, we search for an operational definition of the estimators of the projection coefficients, $\hat{F}_{\mu\alpha}$ and $\hat{\sigma}_{\mu\nu\alpha}^2$. These estimators consists of increment-constructions projected onto the trajectory-dependent orthonormal basis functions, constructed in such a way that the leading order term in Δt converge to the exact projection coefficients. Due to the Gaussian nature of the stochastic noise, this projection procedure – which is equivalent to a least-square regression of the local estimator – corresponds for the force field to a maximum-likelihood approximation [1].

2 Derivation of the discrete estimators

To derive the leading order bias in the estimators for F and σ , we start by defining the increments of the positions:

$$\Delta x_\mu^{(n)}(t) = x_\mu(t + n\Delta t) - x_\mu(t) \quad (\text{S8})$$

The estimator for the accelerations is then given by a linear combination of these increments:

$$\hat{a}_\mu(t) = \frac{\Delta x_\mu^{(2)}(t) - 2\Delta x_\mu^{(1)}(t)}{\Delta t^2} = \frac{x_\mu(t + 2\Delta t) - 2x_\mu(t + \Delta t) + x_\mu(t)}{\Delta t^2} \quad (\text{S9})$$

Note that this is not in general the most natural way to define $\hat{a}_\mu(t)$, as this expression is not centered around t . However, it makes the expression causal: the noise at $t' > t$ is independent of the state at t , thus using forward increments significantly simplifies the calculations. We will later shift the definition back to a centered one, which will only add higher order terms to our results. Similarly, we define the discrete velocity estimator

$$\hat{v}_\mu(t; \lambda) = \frac{\lambda \Delta x_\mu^{(2)}(t)}{2\Delta t} + \frac{(1 - \lambda) \Delta x_\mu^{(1)}(t)}{\Delta t} \quad (\text{S10})$$

Note that we have kept some freedom in how we calculate the velocities from the three points $\{t, t + \Delta t, t + 2\Delta t\}$, denoted by the parameter λ . While most previous approaches [2, 3, 4, 5] use $\lambda = 0$, we will later show that in the presence of measurement noise, we have to choose $\lambda = 1$ (*i.e.* \hat{v} odd under time reversal around $t + \Delta t$) to obtain an unbiased estimator. For now, we keep it as a variable parameter.

2.1 Itô integrals

Throughout this appendix, we will make use of Itô integrals [6], defined as follows:

$$I_0^{(n)} = \int_t^{t+n\Delta t} ds = n\Delta t \quad (\text{S11})$$

$$I_{00}^{(n)} = \int_t^{t+n\Delta t} ds \int_t^s ds' = (n\Delta t)^2 \quad (\text{S12})$$

$$I_\mu^{(n)} = \int_t^{t+n\Delta t} d\tilde{\zeta}_\mu(s) \quad (\text{S13})$$

$$I_{0\mu}^{(n)} = \int_t^{t+n\Delta t} ds \int_t^s d\tilde{\zeta}_\nu(s') \quad (\text{S14})$$

$$I_{\mu\nu}^{(n)} = \int_t^{t+n\Delta t} d\tilde{\zeta}_\mu(s) \int_t^s d\tilde{\zeta}_\nu(s') \quad \text{etc.} \quad (\text{S15})$$

Throughout the text, we will frequently make use of the following identity

$$\langle I_{0\mu}^{(n)} I_{0\nu}^{(m)} \rangle = (\Delta t^3) \delta_{\mu\nu} f_{nm} \quad \text{where} \quad f_{nm} = \begin{cases} 1/3 & n = m = 1 \\ 5/6 & n = 1, m = 2 \\ 8/3 & n = m = 2 \\ 4/3 & n = 1, m = 3 \\ 14/3 & n = 2, m = 3 \\ 9 & n = m = 3 \end{cases} \quad (\text{S16})$$

2.2 Deterministic term

A first intuitive guess for the estimator of the force projections $F_{\mu\alpha}$ are the average projections of the acceleration

$$\hat{A}_{\mu\alpha} = \langle \hat{a}_\mu c_\alpha(\mathbf{x}, \hat{\mathbf{v}}) \rangle \quad (\text{S17})$$

and indeed, this quantity has been used as a proxy for $F_{\mu\alpha}$ throughout the literature [2, 3, 4, 5]. To rigorously derive the leading order contributions to this quantity in terms of the dynamical terms F_μ and $\sigma_{\mu\nu}$, we start by expanding the increments

$$\Delta x_\mu^{(n)} = v_\mu I_0^{(n)} + \int_t^{t+n\Delta t} ds (v_\mu(s) - v_\mu) \quad (\text{S18})$$

$$= v_\mu I_0^{(n)} + \int_t^{t+n\Delta t} ds \left[\int_t^s ds' F_\mu(\mathbf{x}(s'), \mathbf{v}(s')) + \int_t^s d\zeta_\nu(s') \sigma_{\mu\nu}(\mathbf{x}(s'), \mathbf{v}(s')) \right] \quad (\text{S19})$$

$$= v_\mu I_0^{(n)} + \sigma_{\mu\nu} I_{0\nu}^{(n)} + F_\mu I_{00}^{(n)} + (\partial_{v_\rho} \sigma_{\mu\nu}) \sigma_{\rho\tau} I_{0\nu\tau}^{(n)} + \mathcal{O}(\Delta t^{5/2}) \quad (\text{S20})$$

where we defined $v_\mu \equiv v_\mu(t)$, $F_\mu \equiv F_\mu(\mathbf{x}(t), \mathbf{v}(t))$, etc. We will use this short-hand notation as well as the Einstein summation convention throughout.

Next, we expand the basis functions $c_\alpha(\mathbf{x}, \hat{\mathbf{v}})$ around the true velocities \mathbf{v} :

$$c_\alpha(\mathbf{x}, \hat{\mathbf{v}}) = c_\alpha(\mathbf{x}, \mathbf{v}) + (\partial_{v_\rho} c_\alpha)(\hat{v}_\rho - v_\rho) + \frac{1}{2} (\partial_{v_\rho v_\tau}^2 c_\alpha)(\hat{v}_\rho - v_\rho)(\hat{v}_\tau - v_\tau) + \mathcal{O}(\Delta t^{3/2}) \quad (\text{S21})$$

From Eq. (S20), the leading order term of $\hat{v}_\rho - v_\rho$ is given by

$$\hat{v}_\rho - v_\rho = \frac{\lambda}{2\Delta t} \sigma_{\rho\nu} I_{0\nu}^{(1)} + \frac{1-\lambda}{\Delta t} \sigma_{\rho\nu} I_{0\nu}^{(2)} + \mathcal{O}(\Delta t) \quad (\text{S22})$$

Thus, the leading order contribution to the second term of Eq. (S22) is a fluctuating (zero average) term of order $\Delta t^{1/2}$. To evaluate Eq. (S17), we also need the acceleration estimator \hat{a}_μ . Substituting Eq. (S20) into Eq. (S9), we find the leading order terms of the acceleration estimator

$$\hat{a}_\mu = \frac{1}{\Delta t^2} \left[\sigma_{\mu\nu} (I_{0\nu}^{(2)} - 2I_{0\nu}^{(1)}) + F_\mu \Delta t^2 \right] + \mathcal{O}(\Delta t^{3/2}) \quad (\text{S23})$$

Thus, the leading order contribution to the acceleration is a fluctuating (zero average) term of order $\Delta t^{-1/2}$.

When we evaluate Eq. (S17) by substituting Eq. (S20) and (S22), we obtain

$$\hat{A}_{\mu\alpha} = \langle F_\mu c_\alpha(\mathbf{x}, \mathbf{v}) \rangle + \frac{1+2\lambda}{6} \langle (\partial_{v_\rho} c_\alpha(x, v)) \sigma_{\rho\nu} \sigma_{\mu\nu} \rangle + \mathcal{O}(\Delta t) \quad (\text{S24})$$

The second term in this expression is an $\mathcal{O}(\Delta t^0)$ -bias which means that the acceleration projections do not converge to the projections of the force, even in the limit of infinite sampling rate ($\Delta t \rightarrow 0$). This cross-term originates from the product of the fluctuating terms in the basis functions (of order $\Delta t^{1/2}$) and the accelerations (of order $\Delta t^{-1/2}$), which multiplied together give a term of order Δt^0 with non-zero average.

Our expression for the $\mathcal{O}(\Delta t^0)$ -bias has several interesting properties:

- As one might expect, it vanishes in the deterministic limit $\sigma \rightarrow 0$; it is thus a property of stochastic systems.
- It vanishes for purely positional terms in the force-field, as it depends on the derivative $\partial_{v_\rho} c_\alpha(x, v)$. This makes sense, since it originates from the \hat{v} -dependence of the basis functions (Eq. (S22)). As shown by our derivation, it is a consequence of averaging the second derivative of a stochastic signal conditioned on its first derivative.

- A seemingly simple solution to remove the bias would be to set $\lambda = -1/2$. This results in a rather unconventional definition of the discrete velocity estimator,

$$\hat{v}_\mu(t; \lambda = -1/2) = \frac{1}{\Delta t} \left[-\frac{1}{4}x(t+2\Delta t) + \frac{3}{2}x(t+\Delta t) - \frac{5}{4}x(t) \right] \quad (\text{S25})$$

for which $\hat{A}_{\mu\alpha}$ is a convergent estimator of $F_{\mu\alpha}$. However, using this definition of \hat{v}_μ results in large correction terms at the next order in Δt , and thus does not perform well at finite Δt . This estimator would also be strongly biased by measurement noise. For these reasons, we disregard it and turn to the derivation of a better estimator.

For $\lambda \neq -1/2$, the bias does not vanish, and has to be explicitly corrected for. Eq. (S24) allows us to derive an estimator for $F_{\mu\alpha}$ which is unbiased to first order in Δt , *i.e.* which converges to the exact projection coefficients in the limit $\Delta t \rightarrow 0$:

$$\hat{F}_{\mu\alpha} = \langle \hat{a}_\mu c_\alpha(\mathbf{x}, \hat{\mathbf{v}}) \rangle - \frac{1+2\lambda}{6} \left\langle (\partial_{v_\nu} c_\alpha(\mathbf{x}, \hat{\mathbf{v}})) \widehat{\sigma}_{\mu\nu}^2(\mathbf{x}, \hat{\mathbf{v}}) \right\rangle \quad (\text{S26})$$

Note that in going from Eq. (S24) to Eq. (S26), we have replaced v and σ by their estimators, as their values are not known. This introduces additional correction terms, but these are of higher order in Δt . Eq. (S26) further implies that the stochastic term σ^2 has to be inferred before the deterministic term. In the presence of measurement noise (section 3), we show below that we must choose $\lambda = 1$, rendering \hat{v}_μ odd under time reversal around $t + \Delta t$. We therefore use this choice for λ throughout.

Note that Eq. (S26) now conditions the acceleration \hat{a}_μ (Eq. (S9)) on its first point $x(t)$. In order to make this estimator symmetric, we shift the conditioning $c(\mathbf{x}(t), \hat{\mathbf{v}}(t)) \rightarrow c(\mathbf{x}(t + \Delta t), \hat{\mathbf{v}}(t))$. The resulting corrections, due to expanding $c(\mathbf{x}(t + \Delta t), \hat{\mathbf{v}}(t))$ around $\mathbf{x}(t)$, are of higher order in Δt . We can then relabel all time points such that $t \rightarrow t - \Delta t$, to arrive at our final formula for the estimator:

$$\hat{F}_{\mu\alpha} = \langle \hat{a}_\mu c_\alpha(\mathbf{x}, \hat{\mathbf{v}}) \rangle - \frac{1}{2} \left\langle (\partial_{v_\nu} c_\alpha(\mathbf{x}, \hat{\mathbf{v}})) \widehat{\sigma}_{\mu\nu}^2(\mathbf{x}, \hat{\mathbf{v}}) \right\rangle \quad (\text{S27a})$$

$$\mathbf{x} = \mathbf{x}(t) \quad (\text{S27b})$$

$$\hat{\mathbf{v}} = \frac{\mathbf{x}(t + \Delta t) - \mathbf{x}(t - \Delta t)}{2\Delta t} \quad (\text{S27c})$$

$$\hat{\mathbf{a}} = \frac{\mathbf{x}(t + \Delta t) - 2\mathbf{x}(t) + \mathbf{x}(t - \Delta t)}{\Delta t^2} \quad (\text{S27d})$$

2.3 Stochastic term

To derive an estimator for σ , we derive the leading order contributions to the quantity

$$\Delta t \langle \hat{a}_\mu \hat{a}_\nu \hat{c}_\alpha(\mathbf{x}, \hat{\mathbf{v}}) \rangle = \Delta t \langle [\sigma_{\mu\rho} I_{0\rho}^{(2)} - 2\sigma_{\mu\rho} I_{0\rho}^{(1)}] [\sigma_{\nu\rho} I_{0\rho}^{(2)} - 2\sigma_{\nu\rho} I_{0\rho}^{(1)}] c_\alpha(\mathbf{x}, \mathbf{v}) \rangle + \mathcal{O}(\Delta t) \quad (\text{S28})$$

$$= \frac{2}{3} \langle \sigma_{\mu\rho} \sigma_{\nu\rho} c_\alpha(\mathbf{x}, \mathbf{v}) \rangle + \mathcal{O}(\Delta t) \quad (\text{S29})$$

where we have used Eqs. (S16), (S20). Here, the somewhat counter-intuitive factor of 2/3 stems from the expectation values of the Itô-integrals given in Eq. (S16). Thus, an unbiased estimator

to first order in Δt for the stochastic term is

$$\boxed{\widehat{\sigma}_{\mu\nu}^2 = \frac{3\Delta t}{2} \langle \hat{a}_\mu \hat{a}_\nu \hat{c}_\alpha(\mathbf{x}, \hat{\mathbf{v}}) \rangle} \quad (\text{S30})$$

2.4 Comparison to the exact formula for a linear damping force

Pedersen et al. [3] calculated the discretization effect for a linear viscous damping force $F(v) = -\gamma v$ (*i.e.* the one-dimensional inertial Ornstein-Uhlenbeck process), to which we can compare our expression for the $\mathcal{O}(\Delta t^0)$ -bias. The equation of motion for this process is given by

$$\dot{v} = -\gamma v + \sigma \bar{\zeta}(t) \quad (\text{S31})$$

In ref. [3], the acceleration projections

$$\langle \hat{a} | \hat{v} \rangle = -\hat{\gamma} \hat{v} \quad (\text{S32})$$

are considered. Here, $\langle \hat{a} | \hat{v} \rangle$ denotes conditional averaging of \hat{a} with respect to \hat{v} , which is equivalent to using a basis of δ -functions, *i.e.* $b_\alpha(v) = \delta(v - v^{(a)})$. Using our definition of the velocity estimator (Eq. (S10)) with $\lambda = 0$, one obtains [3]

$$\hat{\gamma} = \frac{1}{\Delta t} \left[1 - \frac{(1 - e^{-\gamma \Delta t})^2}{2(e^{-\gamma \Delta t} - 1 + \gamma \Delta t)} \right] \approx \frac{2}{3} \gamma - \frac{5}{18} \gamma^2 \Delta t + \frac{23}{270} \gamma^3 \Delta t^2 + \mathcal{O}(\Delta t^3) \quad (\text{S33})$$

From Eq. (S24), we expect to find a similar bias, since we are considering a v -dependent component of the force field. To compare Eq. (S33) to our result, we use the basis $b = \{v\}$. Then, the normalised projection coefficient is given by

$$c(v) = \frac{v}{\sqrt{\langle v^2 \rangle}} = \frac{\sqrt{2\gamma} v}{\sigma} \quad (\text{S34})$$

since $\langle v^2 \rangle = \sigma^2 / 2\gamma$ for the Ornstein-Uhlenbeck process. Thus, Eq. (S24) predicts

$$\langle \hat{a}_\mu c_\alpha(\hat{v}) \rangle = F_{\mu\alpha} + \frac{(\partial_v c) \sigma^2}{6} + \mathcal{O}(\Delta t) = F_{\mu\alpha} + \frac{\sqrt{2\gamma} \sigma}{6} + \mathcal{O}(\Delta t) \quad (\text{S35})$$

and therefore

$$\langle \hat{a}_\mu c_\alpha(\hat{v}) \rangle c_\alpha(v) = F_\mu + \frac{\gamma}{3} v + \mathcal{O}(\Delta t) = -\frac{2}{3} \gamma v + \mathcal{O}(\Delta t) \quad (\text{S36})$$

Thus, our approach recovers the leading order correction of the expression derived by Pedersen et al. [3].

3 Derivation of estimators in the presence measurement noise

In any real experiment, the recorded positions are subject to measurement noise, due to, e.g., motion blur or uncorrelated localization errors. Such measurement noise can be modelled as an uncorrelated noise $\eta_\mu(t)$ (not necessarily Gaussian) acting on the positions $x_\mu(t)$ [3, 7], meaning that the signal we actually observe is

$$y_\mu(t) = x_\mu(t) + \eta_\mu(t) \quad (\text{S37})$$

where $\langle \eta_\mu(t) \eta_\nu(t') \rangle = \Lambda_{\mu\nu} \delta(t - t')$.

3.1 Deterministic term

We will now again calculate the leading order contributions to the estimator of the projected accelerations:

$$\hat{A}_{\mu\alpha}^{(\text{noisy})} = \langle \hat{a}_{\mu}^{(\text{noisy})} c_{\alpha}(\bar{\mathbf{y}}, \hat{\mathbf{w}}) \rangle \quad (\text{S38})$$

Here, $\hat{\mathbf{a}}^{(\text{noisy})}$ and $\hat{\mathbf{w}}$ are the empirical acceleration and velocity derived from the noisy signal $\mathbf{y}(t)$, respectively. Note that we are no longer conditioning on a single position-like coordinate, but rather the average quantity $\bar{\mathbf{y}}$, which is a linear combination of the three time-points entering the acceleration. This allows us to find a conditioning in terms of $\bar{\mathbf{y}}$ and $\hat{\mathbf{w}}$ such that the leading order terms due to the measurement noise cancel. We thus write

$$\bar{y}_{\mu}(\beta, \gamma) = \beta y_{\mu}(t + 2\Delta t) + \gamma y_{\mu}(t) + (1 - (\beta + \gamma)) y_{\mu}(t + \Delta t) \quad (\text{S39})$$

The noisy velocity estimator for this system is

$$\hat{w}_{\mu} = \hat{v}_{\mu} + \frac{\lambda \Delta \eta_{\mu}^{(2)}}{2\Delta t} + \frac{(1 - \lambda) \Delta \eta_{\mu}^{(1)}}{\Delta t} := \hat{v}_{\mu} + \frac{f_{\mu}^{(v)}(\eta; \lambda)}{\Delta t} \quad (\text{S40})$$

Similarly,

$$\hat{a}_{\mu}^{(\text{noisy})} = \hat{a}_{\mu} + \frac{\Delta \eta_{\mu}^{(2)} - \Delta \eta_{\mu}^{(1)}}{\Delta t^2} := \hat{a}_{\mu} + \frac{f_{\mu}^{(a)}(\eta)}{\Delta t^2} \quad (\text{S41})$$

We assume here that the measurement noise η_{μ} is relatively small compared to the scale of variation of the fitting functions, such that we can expand the basis functions as

$$c_{\alpha}(\bar{\mathbf{y}}, \hat{\mathbf{w}}) = c_{\alpha}(\bar{\mathbf{x}}, \hat{\mathbf{v}}) + (\partial_{x_{\nu}} c_{\alpha}) \bar{\eta}_{\nu}(\beta, \gamma) + (\partial_{v_{\nu}} c_{\alpha}) \frac{f_{\nu}^{(v)}(\eta; \lambda)}{\Delta t} + \mathcal{O}(\eta^2) \quad (\text{S42})$$

Combining Eqs. (S42) and (S41), the estimator of the acceleration projection thus reads

$$\hat{A}_{\mu\alpha}^{(\text{noisy})} = \hat{A}_{\mu\alpha} + (\partial_{x_{\nu}} c_{\alpha}) \frac{\langle \bar{\eta}_{\nu}(\beta, \gamma) f_{\mu}^{(a)}(\eta) \rangle}{\Delta t^2} + (\partial_{v_{\nu}} c_{\alpha}) \frac{\langle f_{\nu}^{(v)}(\eta; \lambda) f_{\mu}^{(a)}(\eta) \rangle}{\Delta t^3} + \mathcal{O}(\eta^2) \quad (\text{S43})$$

This shows that the leading order contribution to the estimator of the acceleration projection is of order Δt^{-3} , inducing a ‘‘dangerous’’ bias which diverges fast with $\Delta t \rightarrow 0$.

Indeed, the standard approach [2, 3, 4, 5] is to take $\hat{A}_{\mu\alpha}^{(\text{noisy})}$ with $\lambda = \beta = \gamma = 0$ as a proxy for the force projections, which results in

$$\hat{A}_{\mu\alpha}^{(\text{noisy})} = \hat{A}_{\mu\alpha} - (\partial_{x_{\nu}} c_{\alpha}) \frac{2\Lambda_{\mu\nu}}{\Delta t^2} - (\partial_{v_{\nu}} c_{\alpha}) \frac{3\Lambda_{\mu\nu}}{\Delta t^3} + \mathcal{O}(\eta^2) \quad (\text{S44})$$

Here we propose to will make use of the free parameters λ , β and γ , to find a construction for our estimator such that the divergent cross-terms in Eq. (S43) cancel. Thus, we solve the following equations for $\{\lambda, \beta, \gamma\}$:

$$\langle \bar{\eta}_{\nu}(\beta, \gamma) f_{\mu}^{(a)}(\eta) \rangle = [(\beta + \gamma) - 2(1 - (\beta + \gamma))] \Lambda_{\mu\nu} \quad (\text{S45})$$

$$\langle f_{\nu}^{(v)}(\eta; \lambda) f_{\mu}^{(a)}(\eta) \rangle = [3\lambda - 3] \Lambda_{\mu\nu} \quad (\text{S46})$$

These terms vanish for $\lambda = 1$ and $\beta + \gamma = 2/3$. There is thus a remaining freedom in the choice of β and γ . For simplicity, we choose the symmetric option $\beta = \gamma = 1/3$. We have thus

determined optimal 'conditioning variables', *i.e.* the arguments $\bar{\mathbf{y}}$ and $\hat{\mathbf{w}}$ of the basis function $c_\alpha(\bar{\mathbf{y}}, \hat{\mathbf{w}})$, that are constructed in such a way that any measurement noise-induced cross-terms cancel.

Thus, an unbiased estimator for the force projections in the presence of measurement noise is

$$\hat{F}_{\mu\alpha}^{(\text{noisy})} = \langle \hat{a}_\mu^{(\text{noisy})} c_\alpha(\bar{\mathbf{y}}(t), \hat{\mathbf{w}}(t)) \rangle - \frac{1}{2} \left\langle (\partial_{v_\nu} c_\alpha(\bar{\mathbf{y}}(t), \hat{\mathbf{w}}(t))) \hat{\sigma}_{\mu\nu}^{2(\text{noisy})}(\bar{\mathbf{y}}(t), \hat{\mathbf{w}}(t)) \right\rangle + \mathcal{O}(\Delta t, \eta^2) \quad (\text{S47a})$$

$$\bar{\mathbf{y}} = \frac{1}{3} (\mathbf{y}(t - \Delta t) + \mathbf{y}(t) + \mathbf{y}(t + \Delta t)) \quad (\text{S47b})$$

$$\hat{\mathbf{w}} = \frac{\mathbf{y}(t + \Delta t) - \mathbf{y}(t - \Delta t)}{2\Delta t} \quad (\text{S47c})$$

$$\hat{\mathbf{a}}^{(\text{noisy})} = \frac{\mathbf{y}(t + \Delta t) - 2\mathbf{y}(t) + \mathbf{y}(t - \Delta t)}{\Delta t^2} \quad (\text{S47d})$$

Clearly, these equations show that to infer the deterministic term, we have to first find an estimator for the stochastic term $\hat{\sigma}_{\mu\nu}^{2(\text{noisy})}$ that is not biased due to measurement noise.

3.2 Stochastic term

To derive an unbiased estimator for the stochastic term in the presence of measurement noise, we follow a very similar line of thought to the derivation of the noisy estimator for the deterministic term. Specifically, using the increments of the process, we derive an estimator constructed such that the bias-terms due to measurement noise $\eta(t)$ vanish. However, in contrast to the estimator for the deterministic term, we now consider an estimator constructed from four points around t , $\{t - \Delta t, t, t + 2\Delta t, t + 3\Delta t\}$. This gives us three increments, rather than two as before, to construct our estimator. This additional freedom is required to construct an estimator that is not spoiled by measurement noise.

As before, we first start by constructing increments of the form

$$\Delta y_\mu^{(n)} = y_\mu(t + n\Delta t) - y_\mu(t) \quad (\text{S48})$$

but now with $n = \{1, 2, 3\}$. We will later transform our results to a notation centered around t . Similar to Eq. (S20), we expand these increments, now including the measurement noise

$$\begin{aligned} \Delta y_\mu^{(n)} &= \Delta x_\mu^{(n)} + \Delta \eta_\mu^{(n)} \\ &= v_\mu I_0^{(n)} + \sigma_{\mu\nu} I_{0\nu}^{(n)} + \Delta \eta_\mu^{(n)} + F_\mu I_{00}^{(n)} + (\partial_{v_\rho} \sigma_{\mu\nu}) \sigma_{\rho\tau} I_{0\nu\tau}^{(n)} + \mathcal{O}(\Delta t^{5/2}) \end{aligned} \quad (\text{S49})$$

Since we are aiming to infer the term $\sigma_{\mu\nu} I_{0\nu}^{(n)}$, which has zero average, we need to consider products of the increments (similar to the noise-free version (S30), where $\hat{\sigma}^2 \sim \hat{a}^2$).

$$\Delta_{\mu\nu}^{(n,m)} := \Delta y_\mu^{(n)} \Delta y_\nu^{(m)} \quad (\text{S50})$$

We thus aim to construct an estimator of the form

$$\Delta t^{-3} \left\langle c_\alpha(\tilde{\mathbf{y}}, \tilde{\mathbf{w}}) \sum_{1 \leq m \leq n \leq 3} k_{mn} \Delta_{\mu\nu}^{(n,m)} \right\rangle \stackrel{!}{=} \sigma_{\mu\nu\alpha}^2 + \mathcal{O}(\Delta t, \eta^2) \quad (\text{S51})$$

We therefore need to find the coefficients k_{mn} for the linear combination of increment products and conditioning coordinates $\tilde{\mathbf{y}}$ and $\tilde{\mathbf{w}}$ such that all dynamical and measurement noise cross-terms except for σ^2 cancel out to first order.

We start by expanding the increment products

$$\begin{aligned} \Delta_{\mu\nu}^{(n,m)} &= v_\mu v_\nu (nm\Delta t^2) + \sigma_{\mu\rho}\sigma_{\nu\tau} I_{0\rho}^{(n)} I_{0\tau}^{(m)} + \Delta\eta_\mu^{(n)} \Delta\eta_\nu^{(m)} + (v_\mu F_\nu m n^2 + v_\nu F_\mu m^2 n)\Delta t^3 \\ &+ (nv_\mu\sigma_{\nu\rho} I_{0\rho}^{(m)} + mv_\nu\sigma_{\mu\rho} I_{0\rho}^{(n)})\Delta t + (mv_\mu\Delta\eta_\nu^{(n)} + nv_\nu\Delta\eta_\mu^{(m)})\Delta t + \mathcal{O}(\Delta t^{7/2}) \end{aligned} \quad (\text{S52})$$

Note that the last two terms in this expansion are zero on average, so one might think that we do not have to include them in the derivation of k_{mn} . This is correct in the case of constant noise. However, in the case of multiplicative noise, these terms correlate with terms in the expansion of the basis function $c_\alpha(\tilde{\mathbf{y}}, \tilde{\mathbf{w}})$, so we have to consider them.

Deriving the coefficients k_{mn} is essentially a linear algebra problem, so we define the vectors

$$\mathbf{d}_{\mu\nu}^{\text{nm}} = \left(\Delta_{\mu\nu}^{(1,1)}, \Delta_{\mu\nu}^{(2,2)}, \Delta_{\mu\nu}^{(3,3)}, \Delta_{\mu\nu}^{(1,3)}, \Delta_{\mu\nu}^{(2,3)}, \Delta_{\mu\nu}^{(1,2)} \right)^T \quad (\text{S53})$$

$$\mathbf{k}^{\text{nm}} = (k_{11}, k_{22}, k_{33}, k_{13}, k_{23}, k_{12})^T \quad (\text{S54})$$

$$\mathbf{t}_{\mu\nu} = \left(v_\mu v_\nu \Delta t^2, \sigma_{\mu\nu}^2 \Delta t^3, \Lambda \delta_{\mu\nu}, F_\mu v_\nu \Delta t^3, v_\mu \sigma_{\nu\rho} I_{0\rho}^{(1)}, v_\mu \sigma_{\nu\rho} I_{0\rho}^{(2)}, v_\mu \sigma_{\nu\rho} I_{0\rho}^{(3)} \right)^T \quad (\text{S55})$$

Note, that in the definition of $\mathbf{t}_{\mu\nu}$ we have temporarily discarded the symmetry under exchange of μ, ν for simplicity. We will later symmetrize our results to regain this symmetry. Furthermore, we have discarded the last term in Eq. (S52) in our definition of $\mathbf{t}_{\mu\nu}$. We will ignore this term in our derivation of k_{mn} as we can take care of it through our choice of conditioning coordinates $\tilde{\mathbf{y}}$ and $\tilde{\mathbf{w}}$.

With these definitions, we explicitly evaluate the increment products:

$$\mathbf{d}_{\mu\nu}^{\text{nm}} = \underline{\underline{R}}^T \cdot \mathbf{t}_{\mu\nu} + \mathcal{O}(\Delta t^{7/2}) \quad (\text{S56})$$

where

$$\underline{\underline{R}} = \begin{pmatrix} 1 & 4 & 9 & 3 & 6 & 2 \\ 1/3 & 8/3 & 9 & 4/3 & 14/3 & 5/6 \\ 2 & 2 & 2 & 1 & 1 & 1 \\ 2 & 16 & 54 & 12 & 30 & 6 \\ 2 & 0 & 0 & 3 & 0 & 2 \\ 0 & 4 & 0 & 0 & 3 & 1 \\ 0 & 0 & 6 & 1 & 2 & 0 \end{pmatrix} \quad (\text{S57})$$

Thus, a general estimator for the variable V is given by solving the equation

$$\hat{V}_{\mu\nu} = \mathbf{k}^{\text{nm}} \cdot \mathbf{d}_{\mu\nu}^{\text{nm}} \stackrel{!}{=} \boldsymbol{\ell}_V \cdot \mathbf{t}_{\mu\nu} \quad (\text{S58})$$

for \mathbf{k}^{nm} . In our case the two quantities of interest are σ^2 and Λ , as we may also wish to infer the amplitude of the measurement noise from the data. The constraint vectors $\boldsymbol{\ell}_V$ for these quantities are given by

$$\boldsymbol{\ell}_{\sigma^2} = (0, 1, 0, 0, 0, 0)^T \quad (\text{S59})$$

$$\boldsymbol{\ell}_\Lambda = (0, 0, 1, 0, 0, 0)^T \quad (\text{S60})$$

So far, we have derived everything in "(nm)-space", for increments as defined in Eq. (S48), which has the key advantage that they are easy to expand. However, for the final form of our estimators, we choose a more natural definition of the increments,

$$\begin{aligned}\Delta y_\mu^{(-)} &= y_\mu(t + \Delta t) - y_\mu(t) \\ \Delta y_\mu^{(0)} &= y_\mu(t + 2\Delta t) - y_\mu(t + \Delta t) \\ \Delta y_\mu^{(+)} &= y_\mu(t + 3\Delta t) - y_\mu(t + 2\Delta t)\end{aligned}\tag{S61}$$

For this "(+-)-space", we define, similarly to before,

$$\mathbf{d}_{\mu\nu}^{+-} = \left(\Delta_{\mu\nu}^{(0,0)}, \Delta_{\mu\nu}^{(-,-)}, \Delta_{\mu\nu}^{(+,+)}, \Delta_{\mu\nu}^{(+,-)}, \Delta_{\mu\nu}^{(0,+)}, \Delta_{\mu\nu}^{(0,-)} \right)^T\tag{S62}$$

$$\mathbf{k}^{+-} = (k_{00}, k_{--}, k_{++}, k_{+-}, k_{0+}, k_{0-})^T\tag{S63}$$

We can transform between the two spaces using

$$\mathbf{d}_{\mu\nu}^{\text{nm}} = \underline{\underline{M}} \mathbf{d}_{\mu\nu}^{+-}\tag{S64}$$

with the transformation matrix

$$\underline{\underline{M}} = \begin{pmatrix} 0 & 1 & 0 & 0 & 0 & 0 \\ 1 & 1 & 0 & 0 & 0 & 2 \\ 1 & 1 & 1 & 2 & 2 & 2 \\ 0 & 1 & 0 & 1 & 0 & 1 \\ 1 & 1 & 0 & 1 & 1 & 2 \\ 0 & 1 & 0 & 0 & 0 & 1 \end{pmatrix}\tag{S65}$$

Thus, we need to solve the transformed equation

$$\underline{\underline{Q}} \mathbf{k}^{+-} = \ell_V\tag{S66}$$

where $\underline{\underline{Q}} = \underline{\underline{R}}(\underline{\underline{M}}^T)^{-1}$. Finally, we add two additional constraints to the matrix $\underline{\underline{Q}}$ which ensure that the final estimator is symmetric in the increments,

$$\underline{\underline{Q}}_{\text{sym}} \mathbf{k}_{\text{sym}}^{+-} = \ell_V^{\text{sym}}\tag{S67}$$

We can now solve for the coefficients:

$$\mathbf{k}_{\text{sym}}^{+-} = \underline{\underline{Q}}_{\text{sym}}^\dagger \ell_V^{\text{sym}}\tag{S68}$$

where $\underline{\underline{Q}}_{\text{sym}}^\dagger$ is the Moore-Penrose pseudoinverse of the non-square matrix $\underline{\underline{Q}}_{\text{sym}}$. This yields

$$\mathbf{k}_{\text{sym}}^{+-}(\sigma^2) = \frac{6}{11}(-1, 1, 1, -6, 1, 1)^T\tag{S69}$$

$$\mathbf{k}_{\text{sym}}^{+-}(\Lambda) = \frac{1}{44}(10, 1, 1, 8, -10, -10)^T\tag{S70}$$

With this solution for the coefficients, the estimator for σ^2 is now operational for the case of constant noise. The estimator for Λ is valid equally in the case of multiplicative noise.

As we noted before, in the case of multiplicative noise, we need to adjust the conditioning variables \tilde{y} and \tilde{x} in order to avoid divergent biases due to the last term in Eq. (S52), similar to

the case of the deterministic term. As our estimator is a four-point construct, we also construct the conditioning variables from four points:

$$\tilde{y}_\mu = \sum_{n=0}^3 a_n y_\mu(t + n\Delta t) = \tilde{x}_\mu + \tilde{\eta}_\mu(\{a_n\}) \quad (\text{S71})$$

$$\tilde{w}_\mu = \frac{1}{\Delta t} \left[b_1 \Delta y_\mu^{(-)} + b_2 \Delta y_\mu^{(0)} + b_3 \Delta y_\mu^{(+)} \right] = \tilde{v}_\mu + \frac{g_\mu^{(v)}(\eta, \{b_n\})}{\Delta t} \quad (\text{S72})$$

where $\sum_{n=0}^3 a_n = \sum_{n=1}^3 b_n = 1$. Similarly to before (Eq. (S42)), we expand the basis functions

$$c_\alpha(\tilde{\mathbf{y}}, \tilde{\mathbf{w}}) = c_\alpha(\tilde{\mathbf{x}}, \tilde{\mathbf{v}}) + (\partial_{x_\nu} c_\alpha) \tilde{\eta}_\nu(\{a_n\}) + (\partial_{v_\nu} c_\alpha) \frac{g_\nu^{(v)}(\eta, \{b_n\})}{\Delta t} + \mathcal{O}(\eta^2) \quad (\text{S73})$$

The remaining bias in our estimator (Eq. (S51)) is due to the last term in Eq. (S52),

$$q_{\mu\nu}^{(m,n)} = (m v_\mu \Delta \eta_\nu^{(n)} + n v_\nu \Delta \eta_\mu^{(m)}) \Delta t \quad (\text{S74})$$

We define

$$\mathbf{q}_{\mu\nu}^{\text{nm}} = \left(q_{\mu\nu}^{(1,1)}, q_{\mu\nu}^{(2,2)}, q_{\mu\nu}^{(3,3)}, q_{\mu\nu}^{(1,3)}, q_{\mu\nu}^{(2,3)}, q_{\mu\nu}^{(1,2)} \right)^T \quad (\text{S75})$$

and can thus write

$$\begin{aligned} \Delta t^{-3} \left\langle c_\alpha(\tilde{\mathbf{y}}, \tilde{\mathbf{w}}) \mathbf{k}_{\text{sym}}^{\text{mn}} \cdot \mathbf{d}_{\mu\nu}^{\text{nm}} \right\rangle &= \langle \sigma_{\mu\nu}^2 c_\alpha(\tilde{\mathbf{x}}, \tilde{\mathbf{v}}) \rangle \\ &+ \Delta t^{-3} \left\langle \mathbf{k}_{\text{sym}}^{\text{mn}} \cdot \mathbf{q}_{\mu\nu}^{\text{nm}} \left((\partial_{x_\rho} c_\alpha) \tilde{\eta}_\rho(\{a_n\}) + (\partial_{v_\rho} c_\alpha) \frac{g_\rho^{(v)}(\eta, \{b_n\})}{\Delta t} \right) \right\rangle + \mathcal{O}(\Delta t, \eta^2) \end{aligned} \quad (\text{S76})$$

This shows that the bias terms are of order Δt^{-3} and Δt^{-4} , and thus diverge in the limit $\Delta t \rightarrow 0$. We now need to find coefficients $\{a_n\}$ and $\{b_n\}$ such that

$$\left\langle \mathbf{k}_{\text{sym}}^{\text{mn}} \cdot \mathbf{q}_{\mu\nu}^{\text{nm}} \tilde{\eta}_\rho(\{a_n\}) \right\rangle = 0 \quad (\text{S77})$$

$$\left\langle \mathbf{k}_{\text{sym}}^{\text{mn}} \cdot \mathbf{q}_{\mu\nu}^{\text{nm}} \frac{g_\rho^{(v)}(\eta, \{b_n\})}{\Delta t} \right\rangle = 0 \quad (\text{S78})$$

We start by explicitly evaluating $\mathbf{q}_{\mu\nu}^{\text{nm}}$:

$$\mathbf{q}_{\mu\nu}^{\text{nm}} = \underline{\underline{E}} \cdot \mathbf{h}_\mu \cdot (v_\nu \Delta t) \quad (\text{S79})$$

where

$$\underline{\underline{E}} = \begin{pmatrix} -2 & 2 & 0 & 0 \\ -4 & 0 & 4 & 0 \\ -6 & 0 & 0 & 6 \\ -5 & 0 & 3 & 2 \\ -4 & 3 & 0 & 1 \\ -3 & 2 & 1 & 0 \end{pmatrix} \quad (\text{S80})$$

and

$$\mathbf{h}_\mu = (\eta_\mu(t), \eta_\mu(t + \Delta t), \eta_\mu(t + 2\Delta t), \eta_\mu(t + 3\Delta t))^T. \quad (\text{S81})$$

We first focus on the conditioning of the configurational (position-like) coordinate, *i.e.* solving Eq. (S77). Defining $\mathbf{a} = (a_0, a_1, a_2, a_3)^T$, Eq. (S77) becomes

$$\left\langle \left(\mathbf{k}_{\text{sym}}^{\text{mn}} \cdot \mathbf{q}_{\mu\nu}^{\text{nm}} \right) (\mathbf{a} \cdot \mathbf{h}_\rho) \right\rangle = 0 \quad (\text{S82})$$

Evaluating

$$\mathbf{k}_{\text{sym}}^{\text{mn}} \cdot \mathbf{q}_{\mu\nu}^{\text{nm}} = \underline{\underline{E}}^T \cdot \underline{\underline{M}} \cdot \mathbf{k}_{\text{sym}}^{+-} (\sigma^2) \quad (\text{S83})$$

$$= \frac{1}{11} (-30, 36, 42, -48)^T \quad (\text{S84})$$

shows that Eq. (S77) is solved by

$$\mathbf{a} = \frac{1}{4} (1, 1, 1, 1)^T. \quad (\text{S85})$$

Next, we find the conditioning of the velocity coordinate, *i.e.* solving Eq. (S78). Defining $\mathbf{b} = (b_1, b_2, b_3)^T$, Eq. (S78) becomes

$$\left\langle \left(\mathbf{k}_{\text{sym}}^{\text{mn}} \cdot \mathbf{q}_{\mu\nu}^{\text{nm}} \right) \frac{\mathbf{b} \cdot \underline{\underline{F}} \cdot \mathbf{h}_\rho}{\Delta t} \right\rangle = 0 \quad (\text{S86})$$

where

$$\underline{\underline{F}} = \begin{pmatrix} -1 & 1 & 0 & 0 \\ 0 & -1 & 1 & 0 \\ 0 & 0 & -1 & 1 \end{pmatrix} \quad (\text{S87})$$

are the coefficients of the measurement noise \mathbf{h} in the velocity estimator $\check{\mathbf{w}}$. Evaluating

$$\underline{\underline{F}} \cdot \mathbf{k}_{\text{sym}}^{\text{mn}} \cdot \mathbf{q}_{\mu\nu}^{\text{nm}} = \underline{\underline{F}} \cdot \underline{\underline{E}}^T \cdot \underline{\underline{M}} \cdot \mathbf{k}_{\text{sym}}^{+-} (\sigma^2) \quad (\text{S88})$$

$$= \frac{6}{11} (11, 1, -15)^T \quad (\text{S89})$$

shows that Eq. (S78) is solved by

$$\mathbf{b} = \frac{1}{6} (1, 4, 1)^T. \quad (\text{S90})$$

Summarizing, an unbiased estimator for the projection coefficients of the multiplicative stochastic term in the presence of measurement noise is given by

$$\widehat{\sigma}_{\mu\nu\alpha}^{2(\text{noisy})} = \Delta t^{-3} \left\langle c_\alpha(\tilde{\mathbf{y}}, \check{\mathbf{w}}) \mathbf{k}_{\text{sym}}^{+-} \cdot \mathbf{d}_{\mu\nu}^{+-} \right\rangle \quad (\text{S91a})$$

$$\mathbf{k}_{\text{sym}}^{+-} = \frac{6}{11} (-1, 1, 1, -6, 1, 1)^T \quad (\text{S91b})$$

$$\tilde{\mathbf{y}} = \frac{1}{4} (\mathbf{y}(t - \Delta t) + \mathbf{y}(t) + \mathbf{y}(t + \Delta t) + \mathbf{y}(t + 2\Delta t)) \quad (\text{S91c})$$

$$\check{\mathbf{w}} = \frac{\Delta \mathbf{y}^{(-)} + 4\Delta \mathbf{y}^{(0)} + \Delta \mathbf{y}^{(+)}}{6\Delta t} \quad (\text{S91d})$$

with $\Delta \mathbf{y}^{(+/0/-)}$ as defined by Eq. (S61) and

$$\mathbf{d}_{\mu\nu}^{+-} = \left(\Delta y_\mu^{(0)} \Delta y_\nu^{(0)}, \Delta y_\mu^{(-)} \Delta y_\nu^{(-)}, \Delta y_\mu^{(+)} \Delta y_\nu^{(+)}, \Delta y_\mu^{(+)} \Delta y_\nu^{(-)}, \Delta y_\mu^{(0)} \Delta y_\nu^{(+)}, \Delta y_\mu^{(0)} \Delta y_\nu^{(-)} \right)^T \quad (\text{S92})$$

3.3 Scaling of the inference error with the measurement noise amplitude

To determine the critical measurement noise amplitude at which the estimators fail, we investigate the scaling of the error curves with the observation time interval Δt . We find that the error curves of the estimator without noise correction (section 2.2) collapse with $\sigma\Delta t^{3/2}$, while the curves of the estimator with noise correction (section 3.1) collapse with Δt .

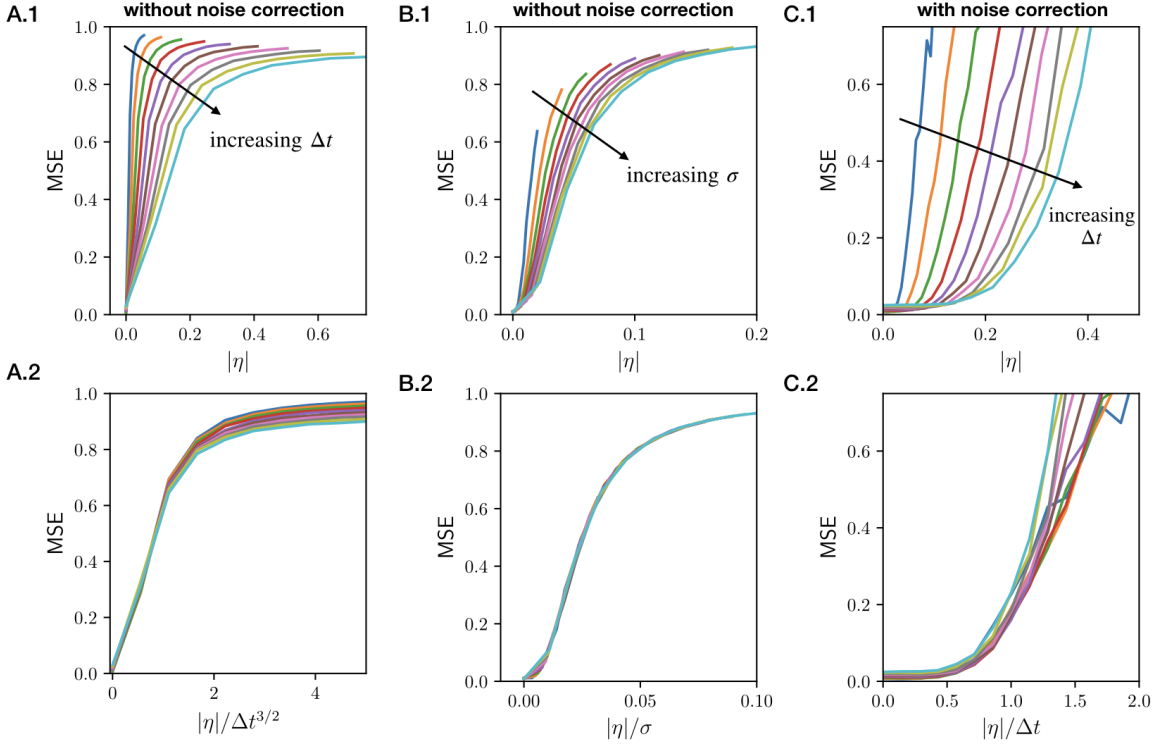


Figure S1: **Error scaling of the force estimator in the presence of measurement noise.** **A.** *Top:* mean-square-error for the estimator without noise correction (section 2.2) as a function of the measurement noise amplitude $|\eta|$ for different values of Δt . *Bottom:* Data collapse by dividing by $\Delta t^{3/2}$. **B.** *Top:* same plot as in B, but for different values of σ . *Bottom:* Data collapse by dividing by σ . **C.** *Top:* mean-square-error along the trajectory for the estimator with noise correction (section 3.1) as a function of the measurement noise amplitude $|\eta|$ for different values of Δt . *Bottom:* Data collapse by dividing by Δt .

4 Inference from experimental single cell trajectories

Here, we discuss the inference from experimental single cell trajectories shown in Fig. 2 of the main text in more detail. Specifically, we show that the experimental trajectories contain enough information to perform inference, and that the inferred models can be inferred self-consistently. Details on cell culture, experimental protocols and tracking procedures can be found in ref. [5].

4.1 Information content of experimental single cell trajectories

As discussed in the main text, the observed trajectories are limited in length due to the finite life-time of a single cell, up until the point where it divides. The expected mean-squared-error in the inferred flow field projected onto a basis b is given by

$$\delta \hat{F}^2 / \hat{F}^2 \sim N_b / 2 \hat{I}_b, \quad (\text{S93})$$

where N_b is the number of degrees of freedom in the basis b , *i.e.* the number of fit parameters. \hat{I}_b is the empirical estimate of the information content of the trajectory of length τ , given by

$$\hat{I}_b = \frac{\tau}{2} \hat{\sigma}_{\mu\nu}^{-2} \hat{F}_{\mu\alpha} \hat{F}_{\nu\alpha}, \quad (\text{S94})$$

measured in natural information units ($1 \text{ nat} = 1 / \log 2 \text{ bits}$). We estimate this information by projecting onto a third-order polynomial basis, and find that the average information per trajectory is 94.2 nats (Fig. S2). To perform accurate inference, we need $\hat{I}_b \gg N_b$. In previous work [5, 8], we inferred models averaged over large numbers of cell trajectories using a basis of 30×30 coarse-grained bins, *i.e.* $N_b = 900$. Thus, single-cell inference was not possible with this approach. In contrast, here we use the partial information to guide a principled selection of basis functions, which shows that most of the information is captured by a symmetrised third-order polynomial basis $\{x, v, x^3, x^2v, xv^2, v^3\}$. Thus, we infer $N_b = 6$ parameters and the criterion $\hat{I}_b \gg N_b$ is fulfilled.

4.2 Self-consistency test of the single-cell inference

To test whether the inferred single-cell models are self-consistent, we simulate trajectories based on the inferred dynamics (Fig. S3). These trajectories perform stochastic transitions on a similar time-scale to the experimental trajectories and exhibit similar oscillation loops in the xv -phase space (Fig. S3E,F). To test model stability, we simulate trajectories of the same length as the experimental ones and sample at the same time interval as in experiment ($\Delta t = 10 \text{ min}$). From these trajectories, we then infer a bootstrapped flow field, which exhibits similar qualitative features as the original flow field inferred from experiments (Fig. S3G). To quantify this, we directly compare the values of the bootstrapped $F(x, v)$ relative to the experimentally inferred $F(x, v)$ along the experimental trajectory (Fig. S3H), which shows strong correlation with a typical mean-squared-error of order 0.3. Thus, SIFI with a symmetrised third-order polynomial basis provides robust, self-consistent models for single-cell trajectories.

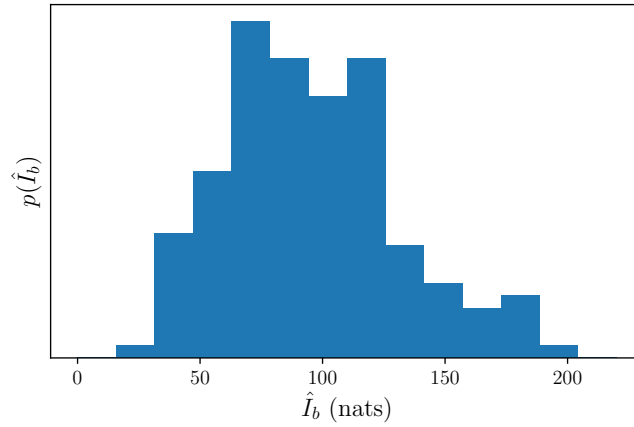


Figure S2: **Information content of single cell trajectories.** Histogram of the information content \hat{I}_b of $N = 149$ single cell trajectories, obtained by projecting onto a third-order polynomial basis. The information is measured in natural information units (1 nat = $1/\log 2$ bits). The average information per trajectory is 94.2 nats.

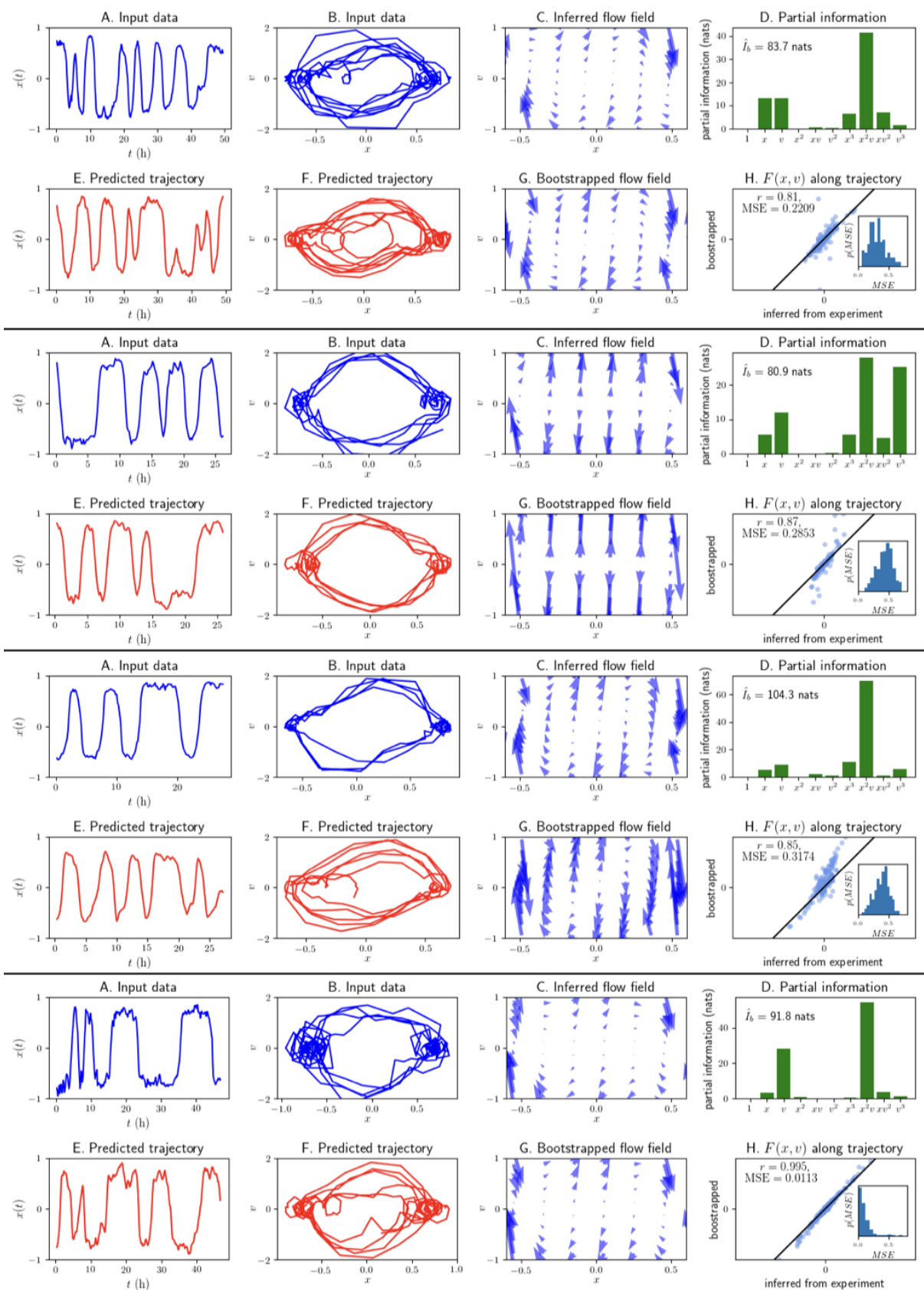


Figure S3: **Inferring single-cell models from two-state migration trajectories.** **A.** Experimentally recorded trajectory of the cell nucleus position, sampled at a time-interval $\Delta t = 10$ min. **B.** xv -plot of the trajectory shown in A. **C.** Flow field inferred from the trajectory in A using SIFI with a symmetrised third-order polynomial basis, $\{x, v, x^3, x^2v, xv^2, v^3\}$. **D.** Partial information of the trajectory shown in A, projected onto a third-order polynomial basis. The total estimated information \hat{I}_b of the trajectory is given. **E.** Trajectory simulated using the inferred model, consisting of the deterministic flow field in C and the inferred constant noise amplitude. The process is simulated at a small time-interval and subsequently sampled at the experimental time-interval $\Delta t = 10$ min. **F.** xv -plot of the simulated trajectory shown in E. **G.** Bootstrapped flow field inferred from the simulated trajectory in E using SIFI with a symmetrised third-order polynomial basis. **H.** Scatter plot of the deterministic term evaluated at the points visited by the experimental trajectory, comparing the flow field inferred from experiment against the bootstrapped result. The mean-squared-error (*MSE*) and the Pearson r -coefficient are given. *Inset:* histogram of the mean-squared-error of $N = 300$ bootstrap realizations. The four sub-figures correspond to four individual cell trajectories. The top subfigure corresponds to the trajectory shown in Fig. 2 of the main text.

5 Model details and simulation parameters for numerical results

To benchmark SIFI, we apply it to several canonical examples of inertial stochastic processes (Fig. 1-3). To simulate these processes, we employ a simple discretization scheme

$$\mathbf{x}(t + dt) = \mathbf{x}(t) + \mathbf{v}(t)dt \quad (\text{S95})$$

$$\mathbf{v}(t + dt) = \mathbf{v}(t) + \mathbf{F}(\mathbf{x}(t), \mathbf{v}(t))dt + \sqrt{dt} \underline{\underline{\sigma}}(\mathbf{x}(t), \mathbf{v}(t)) \cdot \boldsymbol{\zeta}(t) \quad (\text{S96})$$

where $\boldsymbol{\zeta}$ is a vector of independent Gaussian random numbers with zero mean and unit variance. We simulate this equation with a small time interval dt to ensure numerical stability. To generate a realistic experimental position trajectory, we sample the simulated trajectory with a larger interval Δt and add uncorrelated measurement noise to the positions. We use $dt = \Delta t / 20$ throughout. Thus, SIFI only has access to the trajectory

$$\{\mathbf{y}(0), \mathbf{y}(\Delta t), \mathbf{y}(2\Delta t), \dots, \mathbf{y}(\tau - \Delta t), \mathbf{y}(\tau)\} \quad \text{where} \quad \mathbf{y}(t) = \mathbf{x}(t) + \boldsymbol{\eta}(t) \quad (\text{S97})$$

and $\boldsymbol{\eta}$ is a vector of independent Gaussian random numbers with zero mean and unit variance, such that

$$\eta_\mu(t)\eta_\nu(t') = \Lambda\delta_{\mu\nu}\delta(t - t') \quad (\text{S98})$$

and we define $|\boldsymbol{\eta}| = \sqrt{\Lambda}$. The total duration of a trajectory with N_{steps} observation points given by $\tau = N_{\text{steps}}\Delta t$.

5.1 Damped harmonic oscillator (Fig. 1)

We simulate the 1D stochastic damped harmonic oscillator,

$$\dot{v} = -\gamma v - kx + \sigma\zeta \quad (\text{S99})$$

We use $\gamma = k = \sigma = 1$ in all panels. Furthermore, we use Fig. 1A-C: $N_{\text{steps}} = 10^3$, $\Delta t = 0.1$, $|\boldsymbol{\eta}| = 0$

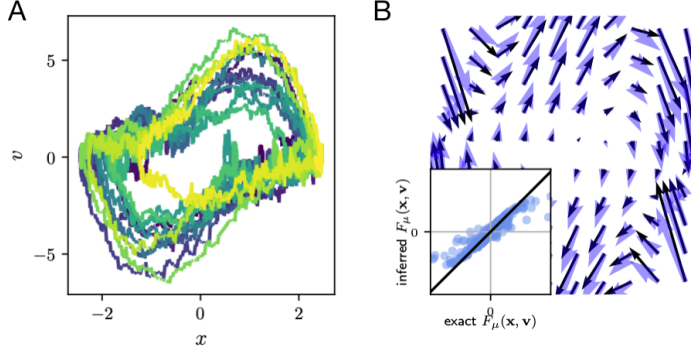


Figure S4: **Inferring Van der Pol dynamics with a Fourier basis.** **A.** Same trajectory as in Fig. 2A in the main text. **B.** SIFI applied to the trajectory in A with basis functions $b = \{\sin(a_x x), \sin(a_v v), \sin(a_x x) \cos(a_v v), \cos(a_x x) \sin(a_v v)\}$. In general, a reasonable choice of the non-linear parameters a_x, a_v is $a_x = 2\pi/L_x, a_v = 2\pi/L_v$, where L_x, L_v are the widths of the sampled phase space in the x and v directions, respectively. From the trajectory in A, we see that $L_x = 6, L_v = 12$ are reasonable choices. *Inset:* inferred components of the force along the trajectory *versus* the exact values.

Fig. 1F-H: $N_{\text{steps}} = 10^3, \Delta t = 0.1, |\eta| = 0.02$

Fig. 1D: $\Delta t = 0.1, |\eta| = 0$

Fig. 1E: $\tau = 10^2, |\eta| = 0$

Fig. 1J: $\Delta t = 0.1, |\eta| = 0.02$

Fig. 1K: $\Delta t = 0.1, N_{\text{steps}} = 10^4$

5.2 Van der Pol oscillator (Fig. 2)

For the Van der Pol oscillator, we use $\mu = 2, \sigma = 1$ throughout.

In Fig. 2A-C, we simulate the 1D Van der Pol oscillator

$$\dot{v} = \mu(1 - x^2)v - x + \sigma\zeta \quad (\text{S100})$$

with $\Delta t = 0.01, N_{\text{steps}} = 10^4, |\eta| = 0.002$. As shown in Supplementary Fig. 1, we recover the dynamics similarly well using a Fourier basis rather than a polynomial basis in the inference.

In Fig. 2 G-J, we simulate the 1D Van der Pol oscillator with multiplicative noise

$$\dot{v} = \mu(1 - x^2)v - x + \sigma(x, v)\zeta \quad (\text{S101})$$

where $\sigma^2(x, v) = \sigma_0 + \sigma_x x^2 + \sigma_v v^2$. We use $\sigma_0 = 1, \sigma_x = 0.3, \sigma_v = 0.1, \Delta t = 0.01, N_{\text{steps}} = 10^4, |\eta| = 0.002$.

5.3 Interacting flocks (Fig. 3)

The model we simulate is a three-dimensional flock of $N = 27$ aligning self-propelled particles, with "soft Lennard-Jones"-type interactions. The particles are initialized on a $3 \times 3 \times 3$ grid with zero velocity. The force on particle i is given by

$$\mathbf{F}_i = \gamma(v_0^2 - |\mathbf{v}_i|^2)\mathbf{v}_i + \sum_{j \neq i} \left[\epsilon_0 \frac{1 - (r/r_0)^3}{(r_{ij}/r_0)^6 + 1} \mathbf{r}_{ij} + \epsilon_1 \exp(-r_{ij}/r_1) \mathbf{v}_{ij} \right] \quad (\text{S102})$$

where $\mathbf{r}_{ij} = \mathbf{r}_j - \mathbf{r}_i$, $\mathbf{v}_{ij} = \mathbf{v}_j - \mathbf{v}_i$, while the noise $\sigma\tilde{\zeta}_i(t)$ on each particle is isotropic and uncorrelated with others. We choose the parameters $\gamma = 1$, $v_0 = 1.5$, $\epsilon_0 = 4$, $r_0 = 2$, $\epsilon_1 = 1$, $r_1 = 3$ and $\sigma = 1$, which result in a flocking behavior similar to that of bird flocks. The simulation is performed with a time step $dt = 0.005$. It is run for 2000 steps to reach steady state before recording, then the trajectory consisting in 1000 time points with time interval $\Delta t = 0.02$ is recorded.

For the inference, we employ a translation-invariant basis with single-particle and pair interaction terms that is invariant under particle exchange $i \leftrightarrow j$, such that

$$F_{i,\mu} \approx F_{\mu\alpha}^{(1)} c_\alpha^{(1)}(\mathbf{v}_i) + F_{\mu\alpha}^{(2)} \sum_{j \neq i} c_\alpha^{(2)}(\mathbf{x}_i - \mathbf{x}_j, \mathbf{v}_i, \mathbf{v}_j) \quad (\text{S103})$$

The single particle fitting functions are chosen to be polynomials of order up to 3 in the velocity (20 functions). The pair interactions are chosen to be of two kinds: radial functions $\sum_j k(r_{ij})\mathbf{r}_{ij}$ and velocity alignment functions $\sum_j k(r_{ij})\mathbf{v}_{ij}$. We choose the same set of fitting kernels $k(r)$ for both radial force and alignment, $k_n(r) = \exp(-r/r_n)$ with $r_n = 0.5n$ and $n = 1 \dots 8$. The outcome of force inference is not very sensitive to this choice; r -dependent Gaussian kernels centered at different radii gives similar results. These result in 8 functions for each component of the vectors \mathbf{r}_{ij} and \mathbf{v}_{ij} , hence 48 functions pair interaction functions. There are thus 68 functions in the basis, and thus 204 fit parameters for the force field. Inferring the diffusion tensor and these fit coefficients, we find that the total information in the trajectory presented in Fig. 3 of the main text is $\hat{I} = 320,000$ nats – more than enough to precisely resolve these parameters. Indeed, we find a mean-squared error on the force of 0.015 along the trajectory; this error could be reduced by adding more functions to the basis.

References

- [1] A. Frishman and P. Ronceray, “Learning force fields from stochastic trajectories,” *Phys. Rev. X*, vol. (in press), p. arXiv:1809.09650, 2020.
- [2] G. J. Stephens, B. Johnson-Kerner, W. Bialek, and W. S. Ryu, “Dimensionality and Dynamics in the Behavior of *C. elegans*,” *PLoS Comput Biol*, vol. 4, no. 4, p. e1000028, 2008.
- [3] J. N. Pedersen, L. Li, C. Grdinaru, R. H. Austin, E. C. Cox, and H. Flyvbjerg, “How to connect time-lapse recorded trajectories of motile microorganisms with dynamical models in continuous time,” *Physical Review E*, vol. 94, no. 6, p. 062401, 2016.
- [4] F. Ferretti, V. Chardès, T. Mora, A. M. Walczak, and I. Giardina, “Building general Langevin models from discrete data sets,” *arXiv:1912.10491*, 2019.
- [5] D. B. Brückner, A. Fink, C. Schreiber, P. J. F. Röttgermann, J. O. Rädler, and C. P. Broedersz, “Stochastic nonlinear dynamics of confined cell migration in two-state systems,” *Nature Physics*, vol. 15, no. 6, pp. 595–601, 2019.
- [6] P. Kloeden and E. Platen, *Numerical Solution of Stochastic Differential Equations*. Springer, 1992.
- [7] C. L. Vestergaard, J. N. Pedersen, K. I. Mortensen, and H. Flyvbjerg, “Estimation of motility parameters from trajectory data: A condensate of our recent results,” *European Physical Journal: Special Topics*, vol. 224, no. 7, pp. 1151–1168, 2015.

- [8] D. B. Brückner, A. Fink, J. O. Rädler, and C. P. Broedersz, "Disentangling the Behavioural Variability of Confined Cell Migration," *J. R. Soc. Interface*, vol. 17, p. 20190689, 2020.